



Universiteit
Leiden
The Netherlands

The role of microRNA alterations in post-ischemic neovascularization

Kwast, R.V.C.T. van der

Citation

Kwast, R. V. C. T. van der. (2020, October 15). *The role of microRNA alterations in post-ischemic neovascularization*. Retrieved from <https://hdl.handle.net/1887/137728>

Version: Publisher's Version

License: [Licence agreement concerning inclusion of doctoral thesis in the Institutional Repository of the University of Leiden](#)

Downloaded from: <https://hdl.handle.net/1887/137728>

Note: To cite this publication please use the final published version (if applicable).

Cover Page



Universiteit Leiden

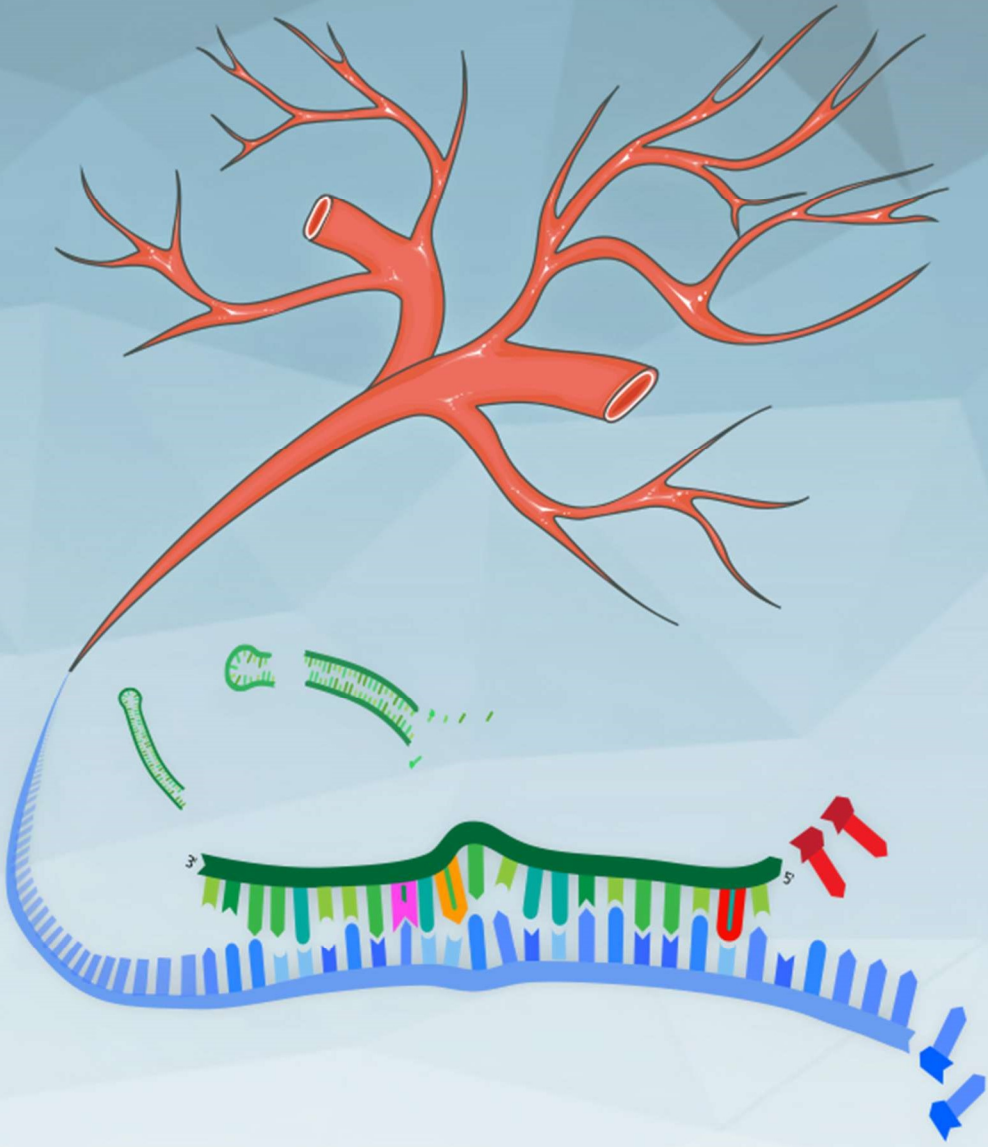


The handle <http://hdl.handle.net/1887/137728> holds various files of this Leiden University dissertation.

Author: Kwast, R.V.C.T. van der

Title: The role of microRNA alterations in post-ischemic neovascularization

Issue Date: 2020-10-15



CHAPTER 5

Adenosine-to-Inosine editing of vasoactive microRNAs alters their targetome and function in ischemia

Reginald V.C.T. van der Kwast

Laura Parma

M. Leontien van der Bent

Eva van Ingen

Fabiana Baganha

Hendrika A.B. Peters

Eveline A.C. Goossens

Karin H. Simons

Meindert Palmen

Margreet R. de Vries

Paul H.A. Quax

A. Yaël Nossent

ABSTRACT

Adenosine-to-inosine (A-to-I) editing in the seed sequence of microRNAs can shift the microRNAs' targetomes and thus their function. Using public RNA-sequencing data, we identified 35 vasoactive microRNAs that are A-to-I edited. We quantified A-to-I editing of the primary (pri-)microRNAs in vascular fibroblasts and endothelial cells. Nine pri-microRNAs were indeed edited, and editing consistently increased under ischemia. We determined mature microRNA editing for the highest expressed microRNAs, i.e., miR-376a-3p, miR-376c-3p, miR-381-3p, and miR-411-5p. All four mature microRNAs were edited in their seed sequence. We show that both ADAR1 and ADAR2 (adenosine deaminase acting on RNA 1 and RNA 2) can edit pri-microRNAs in a microRNA-specific manner. MicroRNA editing also increased under ischemia *in vivo* in a murine hindlimb ischemia model and *ex vivo* in human veins. For each edited microRNA, we confirmed a shift in targetome. Expression of the edited microRNA targetomes, not the wild-type targetomes, was downregulated under ischemia *in vivo*. Furthermore, microRNA editing enhanced angiogenesis *in vitro* and *ex vivo*.

In conclusion, we show that microRNA A-to-I editing is a widespread phenomenon, induced by ischemia. Each editing event results in a novel microRNA with a unique targetome, leading to increased angiogenesis.

Keywords

microRNA, A-to-I editing, ischemia, peripheral artery disease, angiogenesis, target gene regulation, ADAR, cardiovascular disease

INTRODUCTION

MicroRNAs play an important role in processes involved in cardiovascular disease, including neovascularization, atherosclerosis, hypertension and aneurysm formation¹. MicroRNAs are short non-coding RNAs that inhibit translation of the mRNAs they target through partial-complementary binding. In general, only the binding of nucleotides 2 to 8 from the 5'-end end of the microRNA, a microRNA's seed region, is required to induce target silencing². As a result, microRNAs can target hundreds of mRNAs, allowing them to regulate complex, multifactorial physiological and pathological processes, like cardiovascular disease³. Our group has shown that multiple microRNAs from a single microRNA gene cluster, located on the long arm of human chromosome 14 (14q32), are regulated under ischemia and directly affect restoration of blood flow to ischemic tissues⁴.

MicroRNAs are produced after a series of maturation steps of the primary transcript of microRNA genes (pri-microRNAs)². Pri-microRNAs fold into hairpin shaped, double-stranded RNA structures which are sequentially cleaved by ribonucleases Drosha and Dicer yielding a microRNA duplex. Either side of the duplex can be incorporated into the RNA induced silencing complex to become a functional mature microRNA, which are distinguished as either the microRNA on the 5' or 3' side of the pri-microRNA hairpin (microRNA-5p or -3p)².

However, like other RNA species, microRNA transcripts can also be modified at the nucleotide level. Adenosine-to-inosine (A-to-I) editing is the most prevalent RNA nucleotide modification that changes the sequence of the RNA molecule^{5,6}. The inosine preferentially binds to cytidine and is therefore interpreted as guanosine by the cellular machinery. This form of RNA editing is considered an essential post-transcriptional modification, which is regulated in a tissue- and context-specific manner⁷. In mammals, A-to-I editing is catalyzed by either ADAR1 or ADAR2 (adenosine deaminase acting on RNA 1 and 2), which are abundantly expressed throughout the body⁸.

As ADARs target double-stranded RNA structures of at least 20 nucleotides long, A-to-I editing of microRNAs occurs in the pri-microRNA stage⁸. In fact, previous studies have suggested that at least 16% of all human pri-microRNAs contain sites that may be subject to A-to-I editing^{9,10}. Editing of a pri-microRNA can profoundly

influence microRNA maturation¹¹, and several pri-microRNA editing events were shown to be associated with traits, including plasma HDL levels¹². However, if editing occurs in the seed-sequences of either the microRNA-5p or -3p, editing can completely alter the mature microRNA's target selection, resulting in regulation of a different set of target mRNAs, or 'targetome'¹³.

Recently, we demonstrated that microRNA-editing indeed plays a regulatory role in cardiovascular disease. We showed that the pri-microRNA of miR-487b-3p, a microRNA from the 14q32 cluster, is A-to-I edited in the seed-sequence following ischemia¹⁴. We found that the edited mature microRNA (ED-microRNA) indeed selects a completely different targetome than the unedited 'wildtype' microRNA (WT-microRNA). Because of this switch in targetome, ED-miR-487b-3p promotes angiogenesis and neovascularization, whereas WT-miR-487b-3p does not. These findings demonstrated that microRNA editing can play an important role in the endogenous response to pathological stimuli like ischemia. Whether vasoactive microRNAs besides miR-487b-3p are also subject to A-to-I editing in the vasculature however, is still unknown.

Therefore, in this study, we aimed to identify vasoactive microRNAs which are robustly A-to-I edited in vascular cells and to examine if the expression and editing of these microRNAs is regulated under ischemic conditions. Next we aimed to validate our findings in a murine hindlimb ischemia model and subsequently in human vascular tissue. Finally, we examined how editing affects the function of vascular microRNAs, specifically with regards to angiogenesis.

RESULTS

Identification of potential microRNA editing sites

We identified microRNAs containing adenosines which can be subject to A-to-I editing by manual literature curation, in combination with reanalysis of public microRNA-seq datasets. In total, 60 'editable' mature microRNAs originating from 56 different microRNA genes were found to contain robust, context-dependent A-to-G mismatches, indicative of A-to-I editing (**Supplemental Table I**). 35 of these editable microRNAs (58%), of which the vast majority are located in the 14q32 locus (14 of 35, or 40%), could be linked to vascular functions. These 35 vasoactive microRNAs contain a

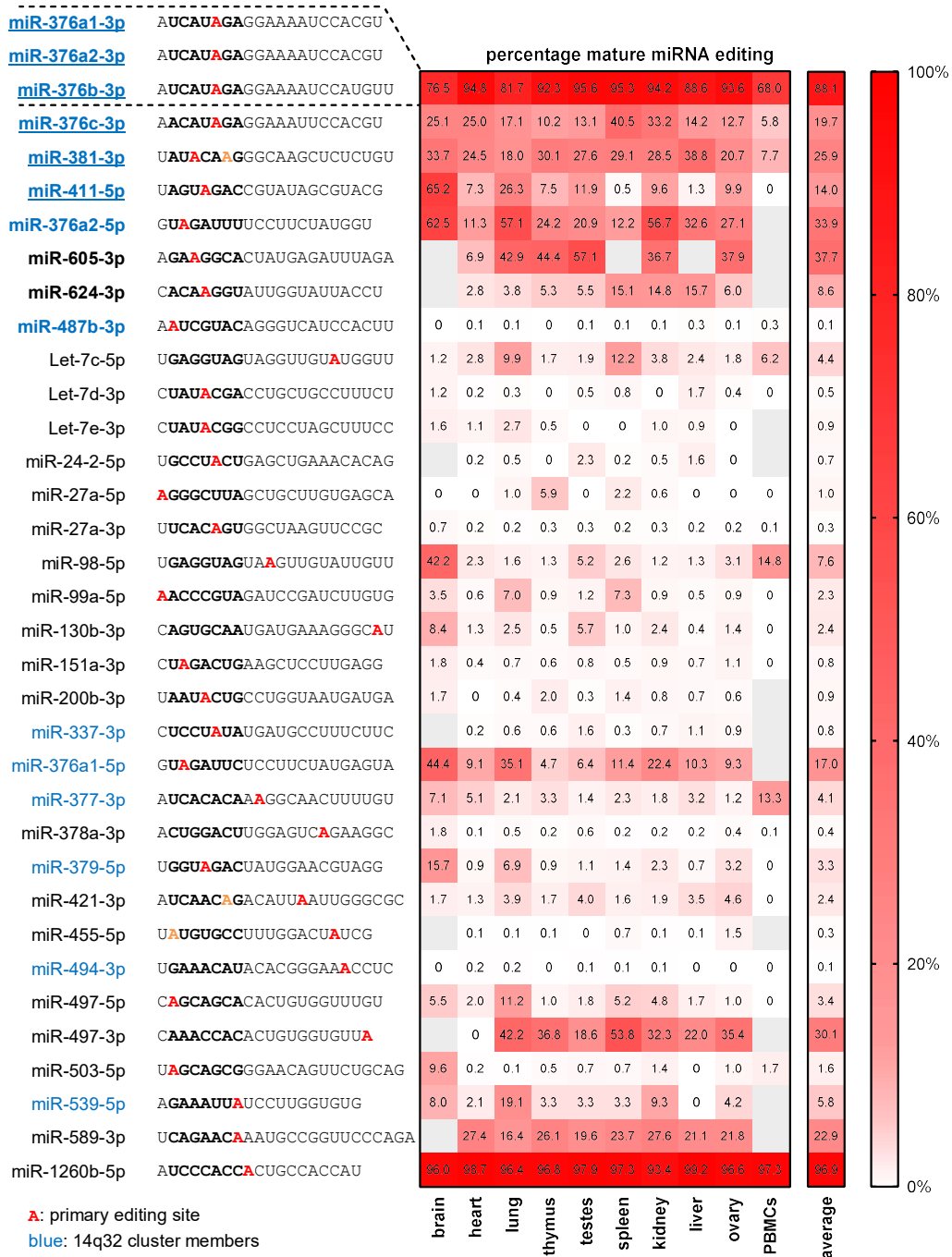
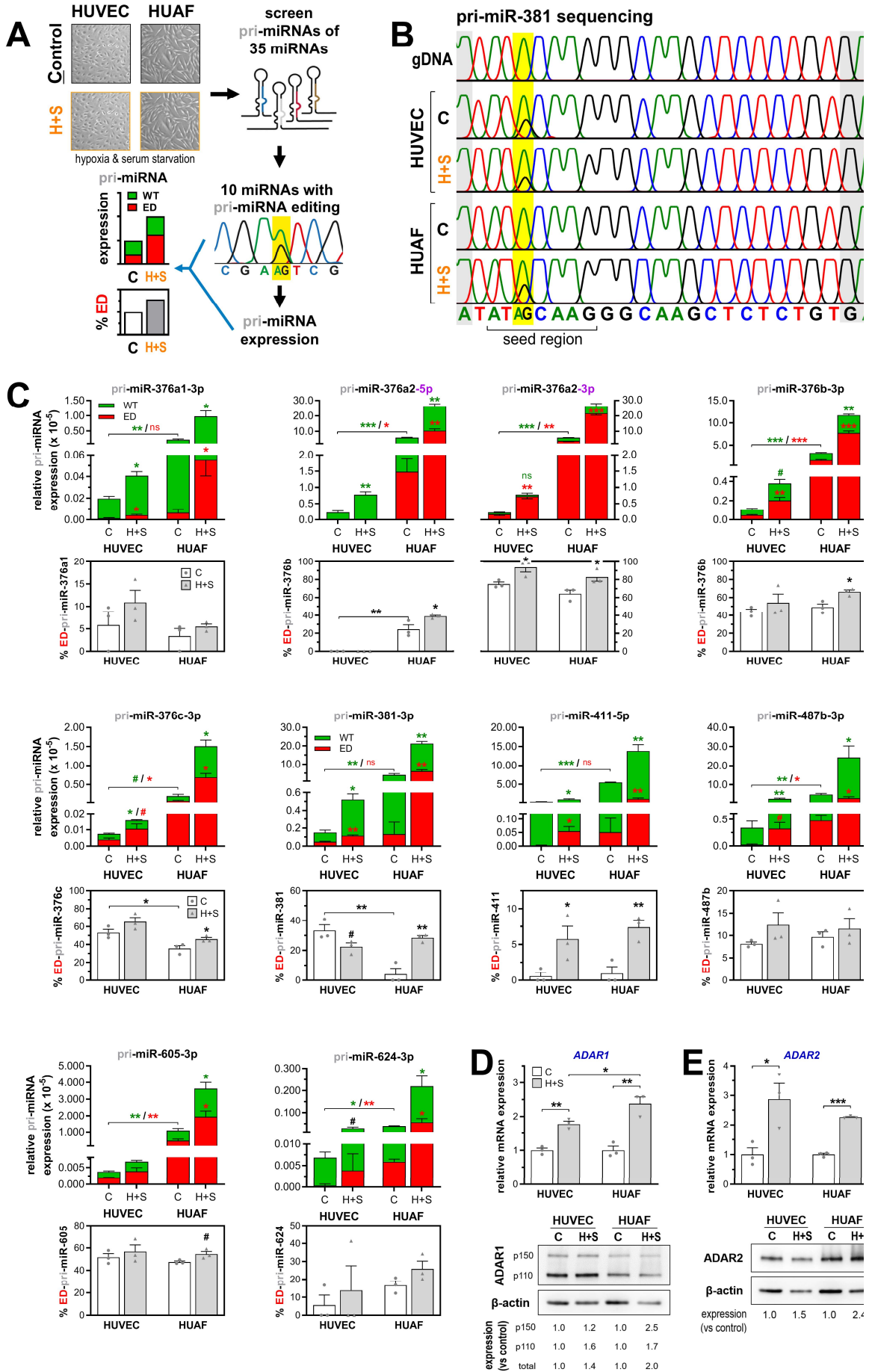


Figure 1: Vasoactive mature microRNAs containing A-to-G mismatches indicative of A-to-I editing. Heatmap displaying percentage A-to-I editing in human tissues of the 35 vasoactive mature microRNAs that were identified to contain potential microRNA editing sites after manual literature curation in combination with reanalysis of public microRNA-seq datasets. Percentage A-to-I editing was obtained by reanalysis of selected high-quality public datasets (n=1) and quantification of percentage A-to-G mismatches, indicative of A-to-I editing. Due to their near complete sequence homology, editing of miR-376a1-3p, miR-376a2-3p and miR-376b-3p editing could not be calculated separately, so their overall percentage editing was presented instead. Gray squares indicate insufficient reads (<10). The location of the quantified editing within the microRNA’s sequence are highlighted in red, while the microRNAs seed-sequence is in bold. Adenosines highlighted in orange were edited to a lower extent than the microRNA’s primary editing site. MicroRNAs in blue are members of the 14q32 microRNA cluster. PBMCs, peripheral blood monocytes.



total of 38 possible editing locations, which display a wide range of percentage A-to-I editing across major human organs (**Figure 1**). The majority of these potential vasoactive mature microRNA editing locations are within the dominantly expressed mature microRNA of the microRNA gene (25 of 38, 66%) and they are localized within the mature microRNA's seed-sequence (26 of 38, 68%).

MicroRNA editing in vascular cells

Both endothelial cells and adventitial fibroblasts are known to play crucial roles in cardiovascular pathology and angiogenesis.¹⁵ Therefore, we determined whether these vasoactive microRNAs are also edited in human umbilical vascular endothelial cells (HUVECs) and human umbilical arterial fibroblasts (HUAFs), cultured either under normal conditions or a combination of hypoxia and serum starvation (hypoxia+starvation) to mimic ischemic conditions (**Figure 2A**). Measurements of HIF1A, VEGFA and p53 expression and visual inspection of the cells validated that the culture conditions successfully induced hypoxia signaling and cell cycle arrest in both HUVECs and HUAFs (**Supplemental Figure I A-D**).

◀ **Figure 2: Identification of A-to-I editing within vasoactive pri-microRNAs and regulation of expression and editing under conditions that mimic ischemia.** (A) Schematic overview detailing the screening of pri-microRNA A-to-I editing in vascular cells. Human umbilical venous endothelial cells (HUVECs) and human umbilical arterial fibroblasts (HUAFs) were cultured separately under “control” conditions (C) or hypoxia+starvation (H+S) to mimic ischemia. Complementary DNA (cDNA) from these cells was subsequently used to screen the 35 selected vasoactive microRNAs for A-to-I editing by sanger sequencing. Percentage pri-microRNA editing quantified from sequencing chromatograms and qPCR quantification of total pri-microRNA expression were used to calculate relative expression of edited pri-microRNAs. (B) Representative chromatograms obtained by sequencing of pri-miR-381. A-to-I RNA editing sites were detected as an A-to-G change in the cDNA sequencing chromatogram, while being absent in the genomic DNA (gDNA) chromatogram. Location of editing within the microRNA's seed region is highlighted in yellow. (C) Expression of unedited (WT) and edited (ED) pri-microRNA expression relative to U6 (top panels) and percentage pri-microRNA editing (bottom panels). (D-E) Fold change in relative ADARI (D) and ADAR2 (E) mRNA and protein expression upon culturing under hypoxia+starvation conditions. In the ADARI western blot, 2 isoforms are visible, known as p150 and p110. Expression both ADARs was normalized to stable household genes RPLP0 or beta-actin (for mRNA and protein expression respectively) and expressed as fold change of the CAD group. All data are presented as mean \pm SEM from 3 independent experiments performed with pooled cells from a total of 13 different umbilical cords. # $P < 0.01$, * $P < 0.05$, ** $P < 0.01$, *** $P < 0.001$; versus control condition unless otherwise indicated by 2-sided Student *t* test.

Screening of each of the selected pri-microRNAs revealed that 10 vasoactive microRNAs (29%), miR-376a1-3p, miR-376a2-5p and -3p, miR-376b-3p, miR-376c-3p, miR-381-3p, miR-411-5p, miR-605-3p, miR-624-3p and miR-487b-3p were indeed A-to-I edited in human vascular cells (**Figure 2B&C**). Except for pri-miR-605 and pri-miR-624, all edited pri-microRNAs are transcribed from the 14q32 microRNA mega-cluster. Each detected vascular pri-microRNA A-to-I editing location corresponds with one of the potential microRNA editing sites which we identified previously. Strikingly, each editing event is located within the microRNA's seed-sequence and all edited microRNAs, except for miR-376a2-5p and miR-624-3p, represent the dominant microRNA of the precursor microRNA duplex, indicating that each editing event is potentially functionally significant. In fact, these edited seed-sequences are different from any other validated microRNA seed-sequence¹⁶ (www.targetscan.org, release 7.2; **Supplemental Table II**).

Pri-microRNA editing

Quantification of pri-microRNA editing and expression revealed that the rate of editing is regulated under hypoxia+starvation (**Figure 2C**). We observed that both pri-microRNA editing and expression generally increase under these culture conditions in both cell types, resulting in a consistent increase in the expression of the edited pri-microRNA (ED-pri-microRNA). An exception to the rule was pri-miR-381, for which the editing rate decreased under hypoxia+starvation from 33% to 22% ($P<0.1$) in HUVECs. In HUAFs however pri-miR-381 editing was induced approximately 6-fold under hypoxia+starvation, as was the editing rate of pri-miR-411 (pri-miR-381: 4.3% to 28%, $P<0.007$ and pri-miR-411: 1.3% to 7.5%, $P<0.02$). The baseline editing rate also differed between HUVECs and HUAFs; pri-miR-376c and pri-miR-381 showed a 1.5-fold and 6-fold higher editing rate in HUVECs compared to HUAFs, respectively, while pri-miR-376a2-5p was only edited in HUAFs (pri-miR-376c: 35.5% vs 53%, $P<0.03$; pri-miR-381: 4.3% vs 27%, $P<0.007$). Baseline pri-microRNA expression was consistently higher and was also induced stronger by hypoxia+starvation in HUAFs than in HUVECs. Combined, these results suggest that regulation of A-to-I editing under ischemic conditions is cell-type specific.

Consistent with these findings, hypoxia+starvation also induced the expression of A-to-I editing enzymes ADAR1 (both p150 and p110 isoforms) and ADAR2, both at mRNA and protein level (**Figure 2D&E**). Protein levels of ADAR1 and ADAR2 increased more in hypoxic+starved HUAFs compared to hypoxic+starved HUVECs (at least 2-fold vs ~1.5-fold induction respectively). Regulation of ADAR expression in response to either serum starvation or hypoxia differed between HUVECs and HUAFs, indicating that ADARs are also regulated in a cell type specific manner (**Supplemental Figure I E&F**).

Mature microRNA editing

To determine whether these edited pri-microRNAs are processed into edited mature microRNAs the four microRNAs with the highest expression were selected: miR-376a-3p (the mature microRNA produced by both pri-miR-376a1 and pri-miR-376a2), miR-376c-3p, miR-381-3p and miR-411-5p (**Supplemental Figure II A**). **Supplemental Table III** provides a comprehensive overview of all our subsequent findings organized per selected microRNA. Expression of 'wildtype', unedited mature microRNA (WT-microRNA) and edited mature microRNA (ED-microRNA) were quantified by version-specific qRT-PCR assays (**Figure 3A**). Due to technical limitations ED-miR-376a-3p could not be distinguished from ED-miR-376b-3p, which has near complete sequence homology, resulting in quantification of their sum instead, ED-miR-376a+b-3p. MiR-376b-3p is generally expressed at 20-fold lower levels than miR-376a-3p (**Figure 3B**). We found that each of the selected edited pri-microRNAs is indeed processed to an edited mature microRNA in both HUVECs and HUAFs. All of these ED-microRNAs, except for ED-miR-376c-3p, have a completely novel seed-sequence (**Figure 3A**) and thus form novel mature microRNAs with a unique targetome.

Mature microRNA editing under ischemic conditions

Baseline mature microRNA expression was consistently higher in HUAFs compared to HUVECs, but percentage mature ED-microRNA was generally lower (**Figure 3B-E**). Percentage ED-miR-376a+b-3p and ED-miR-376c-3p was approximately 60% and 25% respectively, a decrease compared to the percentage editing of pri-miR-376a2-3p and pri-miR-376c-3p in both cell types, suggesting certain edited pri-microRNAs are processed less efficiently than their wildtype counterparts. Despite this, increases in

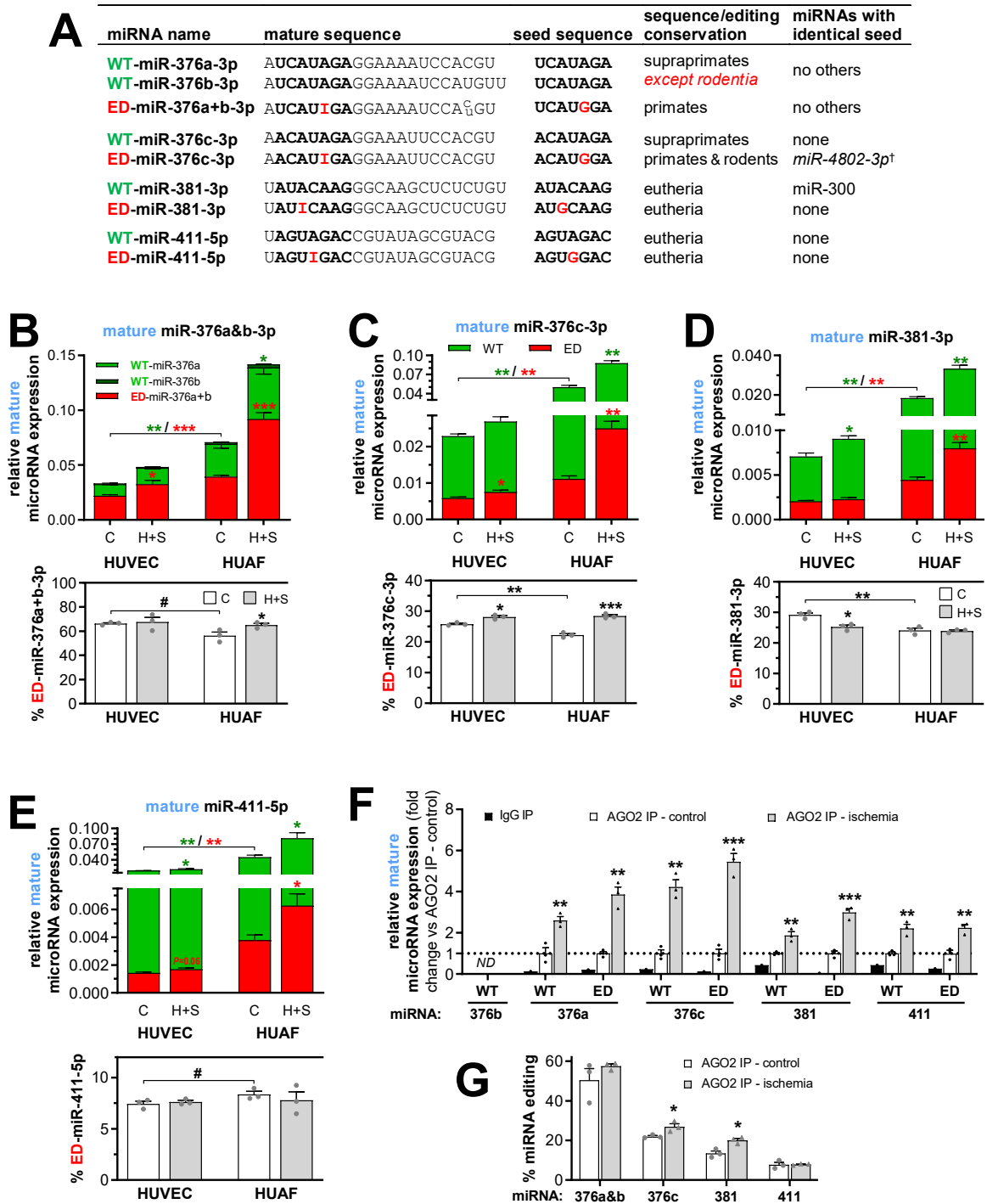


Figure 3: Specific quantification of normal and edited mature microRNAs in vascular cells. (A) Unedited mature microRNAs (WT-microRNA) and edited mature microRNAs (ED-microRNA) were quantified using version specific Taqman qRT-PCR assays. Since inosines resulting from A-to-I editing are recognized as a G, the functional seed-sequence of each microRNA is also highlighted and whether this seed is unique or shared by a different microRNA. [†]unvalidated microRNA according to TargetsScan¹⁶. (B-E) Relative expression of mature WT-microRNA (green) and ED-microRNA (red) in HUVECs and HUAFs cultured in control (C) conditions or hypoxia+starvation (H+S) to mimic ischemia (top panels) and the corresponding percentage mature ED-microRNA (bottom panels). Relative microRNA expression was normalized to U6. (F) Relative expression of WT-microRNAs and ED-microRNAs in fractions after negative control IgG

percentage miR-376a+b-3p and ED-miR-376c-3p during hypoxia+starvation still mirrored changes in percentage pri-microRNA editing. Moreover, consistent with pri-microRNA editing findings, only HUVEC mature miR-381-3p editing decreased with hypoxia+starvation. These aspects of ischemia also consistently induced total mature microRNA expression. As a result, expression of all mature ED-microRNAs also significantly increased under hypoxia+starvation in both HUVECs and HUAFs.

A microRNA has to be associated with an argonaute protein (AGO), the active part of the RNA induced silencing complex, to be functional. To examine if the ED-microRNAs are functional, we performed AGO2-immunoprecipitation on lysates from HUAFs cultured on either normal or hypoxia+starvation conditions and measured the expression of WT-microRNAs and ED-microRNAs in the IP-fractions. Samples from normoxic cells showed enrichment of both WT- and ED-microRNAs in the AGO2 precipitate, compared to an IgG negative control, confirming that both variants of the four investigated microRNAs enter the cell's microRNA-machinery (**Figure 3F**). Conform their increased expression, AGO2 binding of both the WT-microRNA and ED-microRNA variants increased in hypoxic+starved cells. Furthermore, the percentage microRNA-editing increased in the AGO2 precipitates of hypoxic+starved versus normoxic cells for three of the four investigated microRNAs (**Figure 3G**).

ADAR1 and ADAR2 in microRNA expression and editing

To investigate the effect of ADAR1 and ADAR2 on microRNA expression and editing, we used short interfering RNAs (siRNAs) to knockdown ADAR1 or ADAR2 expression in HUAFs (**Supplemental Figure III-A**). Knockdown of either ADAR1 and ADAR2 decreased total pri-microRNA expression by 2- to more than 10-fold compared control siRNA (**Figure 4A**). Furthermore, ADAR1 knockdown resulted in a decrease in pri-microRNA editing for all examined pri-miRs except for pri-miR-376a2. Knockdown of ADAR2 however, only affected editing of pri-miR-376a1 and pri-miR-376a2.

◀ **Figure 3 continued:** ... or AGO2 was immunoprecipitated from HUAFs cultured under control or hypoxia+starvation conditions. Data is expressed as fold change of the control AGO2 immunoprecipitation (IP). (G) Percentage editing measured in AGO2 IP fractions. All data are presented as mean \pm SEM from 3 independent experiments performed with pooled cells from a total of 13 different umbilical cords. # $P < 0.01$, ** $P < 0.05$, *** $P < 0.01$, **** $P < 0.001$; versus control condition unless otherwise indicated by 2-sided Student *t* test. Symbol color shows whether means of either WT or ED expression are compared.

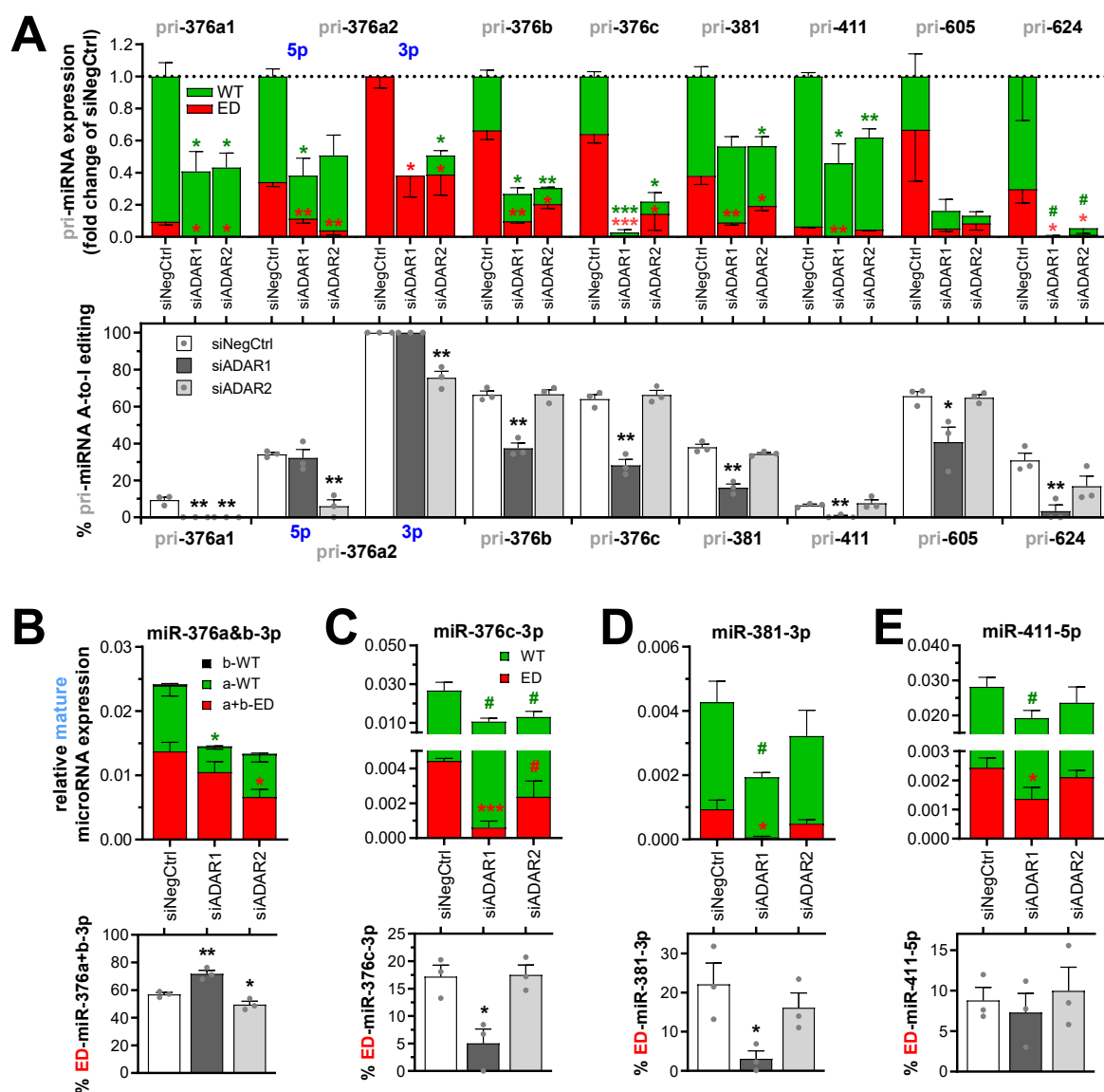


Figure 4: Role of ADAR1 and ADAR2 in vasoactive microRNA editing and maturation. (A-E) ADAR1 and ADAR2 were knocked down in HUAFs through transfection of an *ADAR1*-targeting or *ADAR2*-targeting siRNA (siADAR1 and siADAR2 respectively). The subsequent effects on microRNA expression and editing were analyzed as in **Figure 2&3** and compared to transfection with a negative control siRNA (siNegCtrl). (A) Pri-microRNA A-to-I editing and expression. (B-E) Mature microRNA expression relative to U6 (top panels) and the corresponding percentage mature microRNA-ED (bottom panels). All data are presented as mean \pm SEM from 3 independent experiments performed with pooled cells from 13 different umbilical cords. # $P < 0.01$, * $P < 0.05$, ** $P < 0.01$, *** $P < 0.001$; versus siNegCtrl or as indicated by 2-sided Student *t* test.

Consistent with these findings, mature microRNA expression and editing was similarly affected by the knockdown of ADARs (**Figure 4B-E**). ADAR1 knockdown reduced mature microRNA expression as well as mature microRNA editing for all measured microRNAs, except for editing of miR-376a+b-3p which increased instead.

ADAR2 knockdown also decreased total mature microRNA expression but instead only decreased miR-376a+b editing. Our data suggests that both ADARs play a role in expression of these 14q32 microRNAs, while ADAR1 is responsible for A-to-I editing of all mature microRNAs except for miR-376a-3p.

In vivo microRNA editing

We subjected C57Bl/6 mice to hindlimb ischemia via single ligation of the left femoral artery and measured mature WT-microRNAs and ED-microRNAs in distinct whole-muscle tissues: the adductor which remains relatively normoxic and the gastrocnemius and the soleus which become ischemic¹⁷ (**Figure 5A**). Of the four selected microRNAs, all editing events are conserved in mice except for miR-376a-3p. The seed sequence and editing are not conserved in the murine mmu-miR-376a-3p and therefore mmu-miR-376a was excluded from all experiments using murine tissue. We observed differences in baseline microRNA expression and percentage ED-microRNA between muscle tissues (**Figure 5B**). Furthermore, expression of ED-miR-376c-3p, ED-miR-381-3p and ED-miR-411-5p was increased in the gastrocnemius and soleus muscles 1 day (T1) after HLI compared to before surgery (T0), but not in the adductor muscle. In contrast, at day 3 after surgery (T3) ED-microRNA expression reduced to sub-T0 levels. *Adar1* expression also increased only in the ischemic gastrocnemius and soleus muscles, while *Adar2* expression was induced in all three muscles (**Supplemental Figure III B-D**). These results confirm that vasoactive microRNAs are edited in response to ischemia *in vivo* as well as *in vitro*.

MicroRNA editing in human tissues and vascular disease

To examine whether microRNA expression and editing in human vascular tissue responds similarly to ischemic conditions, we used human venae saphenae magna (VSM) and internal mammary arteries (IMA), which were harvested during elective coronary bypass surgery on patients with coronary artery disease. After culturing the vessels *ex vivo* under control or hypoxia+starvation conditions for 24h, expression and editing of all four selected microRNAs was measured. Prior to this, the IMAs were separated manually into the tunica adventitia and the tunica media/intima, while the VSMs were left intact. Consistent with our *in vitro* and *in vivo* ischemia models,

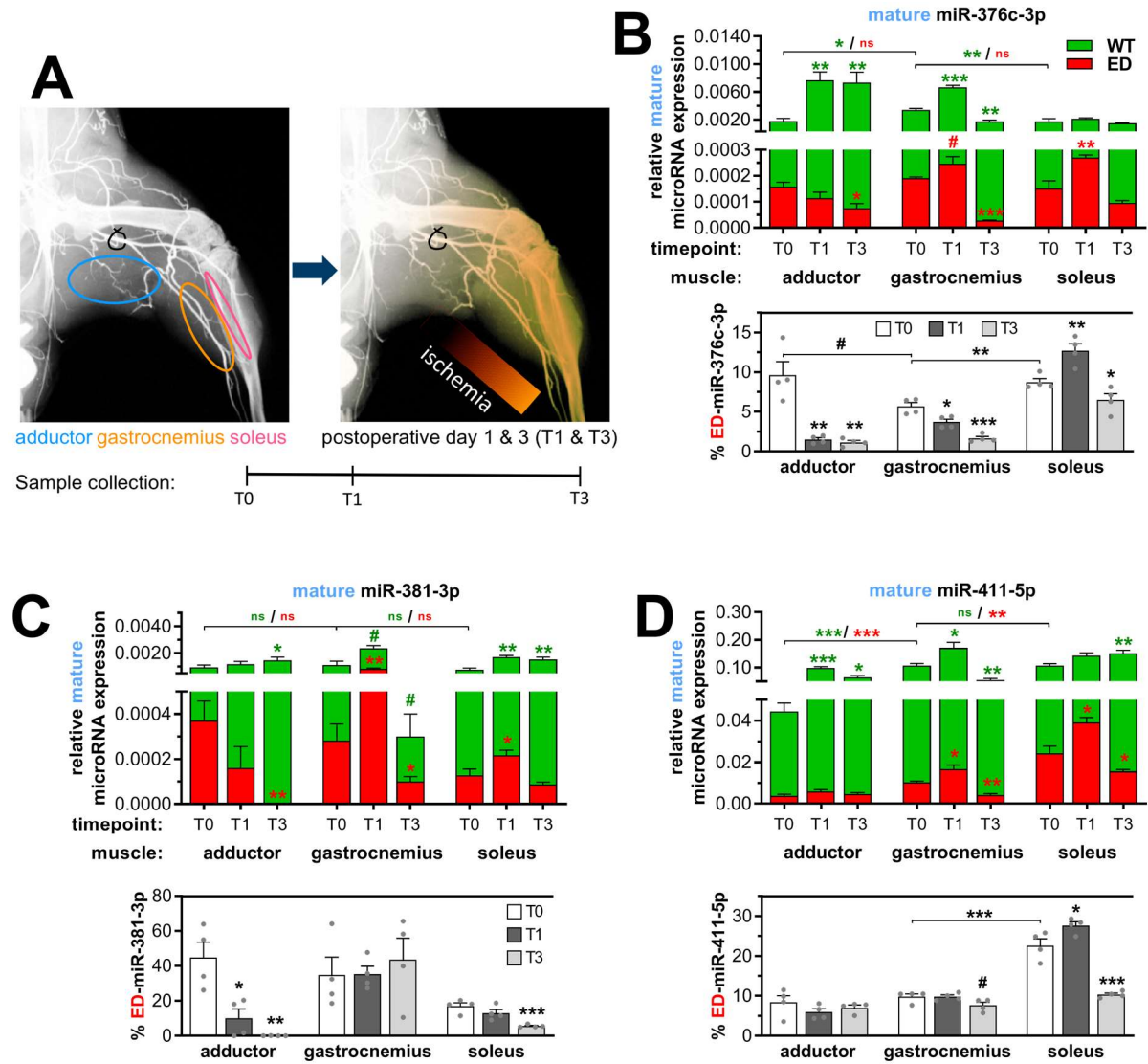


Figure 5: Mature microRNA editing and expression after induction of hindlimb ischemia in muscles experiencing ischemia or increased shear stress (A) Schematic representation of hindlimb ischemia induction by ligation of the femoral artery and the resulting ischemia downstream of the ligation site. Three different muscle tissues were harvested before surgery (T0) or 1 and 3 days after surgery (T1 and T3). While the gastrocnemius and soleus experience ischemia after surgery, the adductor remains relatively normoxic due to its more upstream anatomical location. **(B-D)** Mature microRNA expression relative to U6 (top panels) and the corresponding percentage mature microRNA-ED (bottom panels) in the harvested muscles, presented as in **Figure 3**. All data are presented as mean \pm SEM of muscles harvested from 4 different mice per timepoint. # $P < 0.01$, * $P < 0.05$, ** $P < 0.01$, *** $P < 0.001$; versus T0 unless otherwise indicated by 2-sided Student *t* test. Symbol color shows whether means of either WT or ED expression are compared.

expression of all ED-microRNAs increased significantly after hypoxia+starvation in all vessel segments, except for the adventitia of the IMAs, where trends towards increased expression were observed (**Figure 6A-D**). As before, WT-microRNA expression was

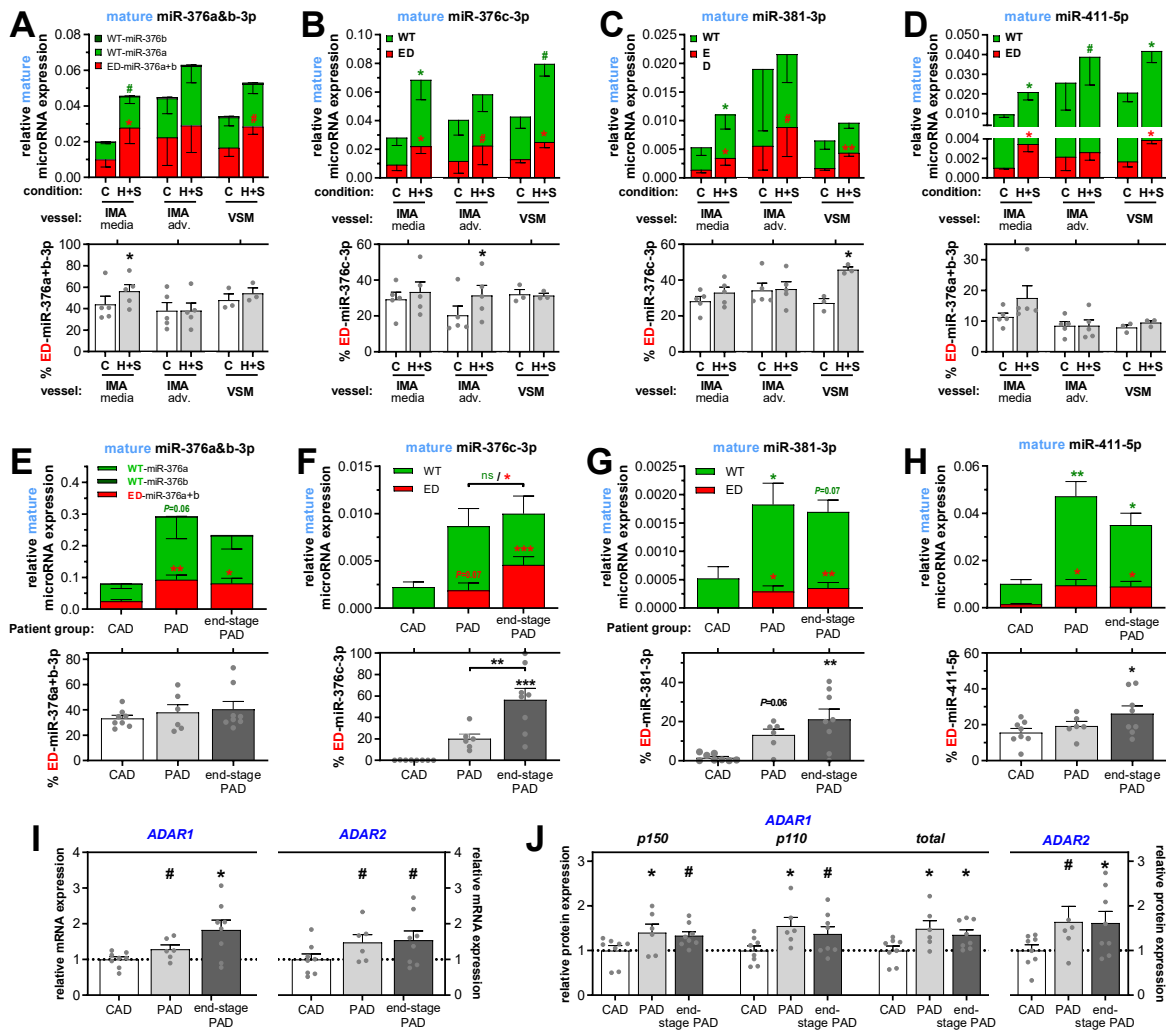


Figure 6: Mature microRNA editing and expression in normoxic and ischemic human vessels (A) MiR-376a+b-3p, (B) miR-376c-3p, (C) miR-381-3p and (D) miR-411-5p expression and editing in internal mammary arteries (IMA, n=5) and vena saphena magna (VSM, n=3) cultured ex vivo control (C) conditions or hypoxia+starvation (H+S) to mimic ischemia. Right before harvest, IMAs were separated manually into the tunica media/intima (media) and the tunica adventitia (adv.) whereas VSMs were left intact. #P<0.01, *P<0.05, **P<0.01, ***P<0.001; versus its TO by paired 2-sided Student t test. Symbol color shows whether means of either WT or ED expression are compared. (E-H) Expression and editing of the same microRNAs in lower leg vein (LLV) samples from three different patient groups with minimal to end-stage peripheral artery disease (PAD). Normoxic LLV samples (n=8) from patients with coronary artery disease (CAD) rather than PAD undergoing coronary artery bypass-surgery were compared to LLV samples (n=6) from patients with severe PAD undergoing femoral artery to popliteal artery-bypass surgery and to LLV samples (n=8) from patients with end-stage PAD, undergoing lower limb amputation. All mature microRNA expressions are normalized to U6. (I&J) Relative ADAR1 and ADAR2 mRNA (I) and protein (J) expression in the LLV samples from different patient groups. Expression was normalized to stable household genes RPLP0 or beta-actin (for mRNA and protein expression respectively) and expressed as fold change of the CAD group. See **Supplemental Figure IV** for the western blots used for the ADAR protein quantification. (E&J) All data are presented as mean ± SEM. *P<0.05, **P<0.01, ***P<0.001; versus TO unless otherwise indicated by one-way ANOVA.

often also increased after hypoxia+starvation treatment. Nevertheless, a significant increase in the percentage editing was observed in at least one of the vessel segments for miR-376a+b-3p, miR-376c-3p and miR-411-5p (IMA adventitia, IMA media and VSM, respectively).

Next, we examined microRNA A-to-I editing in patients with ischemic disease by comparing mature microRNA expression in lower leg vein (LLV) samples from patients with coronary artery disease (CAD) but without clinically actionable peripheral artery disease (PAD) undergoing coronary artery bypass-surgery, to LLV samples from patients with severe PAD undergoing femoral artery to popliteal artery-bypass surgery and to LLV samples from patients with end-stage PAD, undergoing lower limb amputation.

We observed increased expression and editing in LLV tissues from PAD patients compared to CAD patients (**Figure 6E-H**). Of the microRNAs examined, ED-microRNA expression increased by at least 3-fold and only the percentage editing of miR-376a+b-3p remained largely unaffected. We also observed an increase in ADAR1 and ADAR2 mRNA and protein expression in the veins from both PAD and end-stage PAD patients (**Figure 6I&J** and **Supplemental Figure IV**). These data suggest microRNA editing is actively regulated in ischemic disease in humans.

Editing induces a shift in microRNA-targetomes

Since editing of the microRNA resulted in a completely novel seed-sequence for all but one microRNA, changes in putative targetomes of the edited microRNAs were determined using three distinct target prediction algorithms. We found that each WT-microRNA targetome had less than 25% overlap with its respective ED-microRNA targetome. The remaining overlap in targetomes was caused entirely by mRNAs containing two separate binding sites for both the WT-microRNA and the ED-microRNA (**Figure 7A**), rather than single sites that can bind both microRNA variants. In this analysis, the targetomes of miR-376a-3p and miR-376b-3p were combined, as they are nearly identical, both in microRNA sequence and in targetome (more than 95% overlap between individual WT-targetomes and ED-targetomes).

Pathway enrichment analysis of each targetome using the PANTHER algorithm¹⁸ revealed that editing of the selected microRNAs shifts their targetome towards

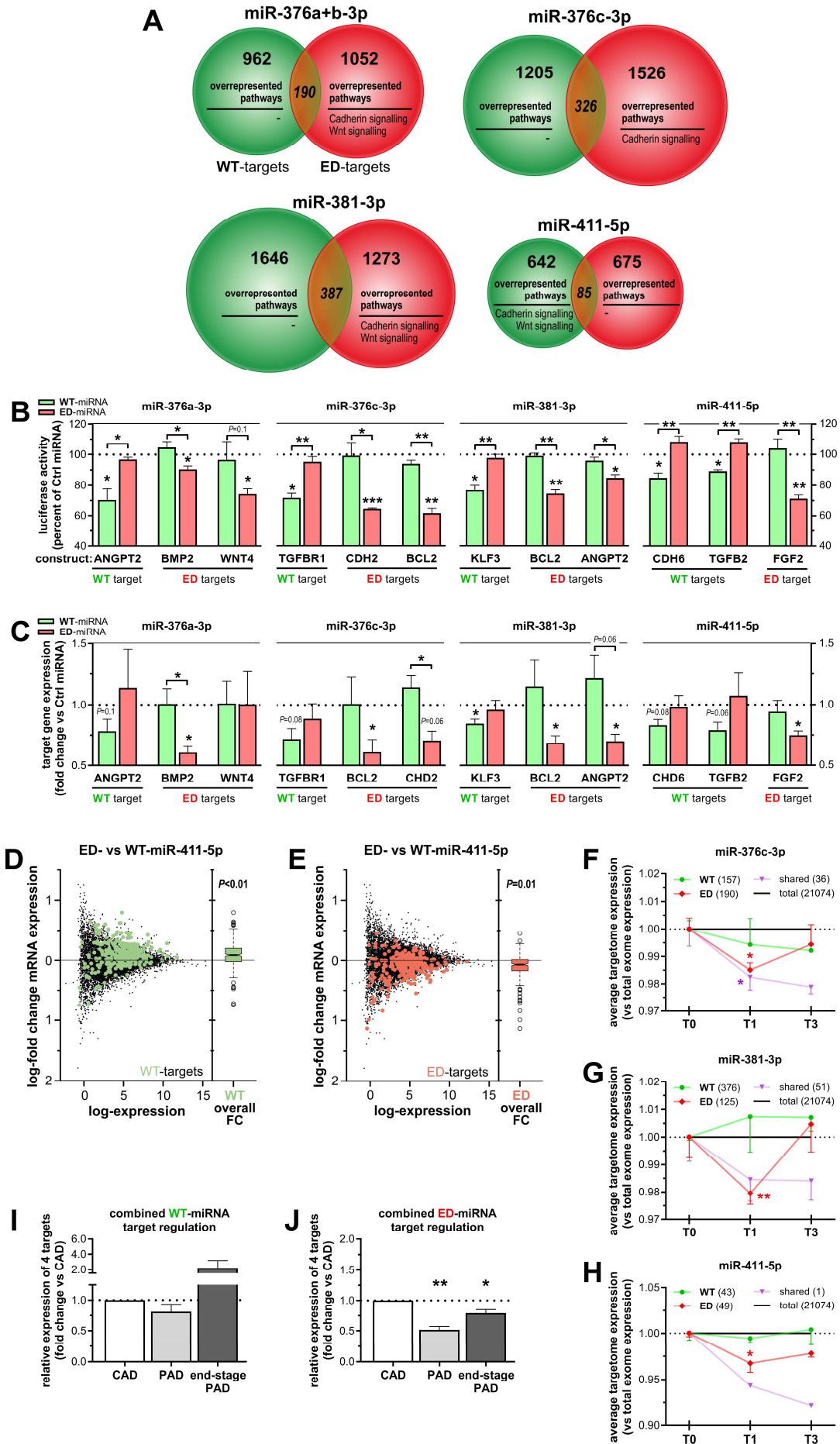
overrepresentation of Cadherin signaling and/or Wnt signaling, with the exception of ED-miR-411-5p, which shifts away from overrepresentation of Cadherin signaling and Wnt signaling (**Figure 7A** and **Supplemental Table IV**).

Genes within each edited targetome could be linked to processes involved in the response to ischemia, including bone morphogenetic protein 2 (BMP2, target of ED-miR-376a+b-3p), Cadherin-2 (CDH2, target of WT-miR-411-5p and ED-miR-376c-3p) and B-cell lymphoma 2 (BCL2, target of ED-miR-376c-3p and ED-miR-381-3p) (**Supplemental Table V**).

Validation of target mRNA regulation

Next we set out to validate whether the single nucleotide change found in each seed-sequence of ED-microRNA indeed causes a shift in target site selection. We performed dual luciferase reporter gene assays using endogenous putative binding sequences from at least one vasoactive target per microRNA (**Figure 7B**). The luciferase activity of the WT-miR-381-3p binding site containing *Krüppel-like factor 3* (*KLF3*) sequence was indeed only repressed by WT-miR-381-3p to $77\pm 3\%$ ($P<0.02$) and not by ED-miR-381-3p ($P=0.7$). Conversely, luciferase activity of the ED-miR-381-3p binding site containing *BCL2* and *Angiopoietin-2* (*ANGPT2*) sequences were only inhibited by ED-miR-381-3p to $74\pm 2\%$ ($P<0.001$) and $85\pm 2\%$ ($P<0.02$) respectively. WT-microRNA versus ED-microRNA specific regulation of vasoactive target sequences was similarly validated for miR-376a-3p, miR-376c-3p and miR-411-5p. These results confirm that each editing event results in a complete shift in target site recognition.

We then overexpressed either the WT-microRNA or ED-microRNA in HUAFs and examined endogenous target mRNA regulation (**Figure 7C**). Consistent with luciferase results, treatment with WT-miR-381-3p decreased endogenous *KLF3* expression by $19\pm 6\%$ ($P=0.05$) but did not affect *BCL2* and *ANGPT2* expression ($P=0.6$ and $P=0.4$ respectively). Treatment with ED-miR-381-3p did not affect *KLF3* expression ($P=0.6$), while expression of both *BCL2* and *ANGPT2* were repressed by 30% ($P>0.04$ for both). Similarly, overexpression of other WT-microRNAs consistently decreased WT targets only. Furthermore, treatment with ED-microRNAs successfully repressed only the ED targets. Only *WNT4* did not appear to be affected by ED-miR-376a-3p in addition to WT-miR-376a-3p, possibly through indirectly being affected by regulation of other ED-



miR-376a-3p targets. Overall, however, average vasoactive target repression by ED-microRNAs was stronger than average target repression by WT-microRNAs ($P < 0.001$, **Supplemental Figure V-E**). This is in line with previous findings for WT- versus ED-miR-487b-3p and could be a consequence of the additional I-C-bond (similar to a G-C-bond) between ED-microRNAs and their target mRNAs, which is stronger than the A-U-bonds between WT-microRNAs and their target mRNAs¹⁴.

◀ **Figure 7: Targetome predictions and validation of target sequence binding and endogenous target regulation** (A) Venn diagram of putative targetomes for WT-microRNA (green) and ED-microRNA (red) representing the putative targets that all three employed prediction algorithms indicated to be targeted. Within each putative targetome, significantly enriched pathways were displayed (see **Supplemental Table IV**). (B) To examine the change in target binding induced by editing, luciferase assays were performed with endogenous microRNA binding sequences from vasoactive targets for either a WT-microRNA or a ED-microRNA as indicated. MicroRNA specific target regulation was assessed by examining luciferase reporter activity after co-transfecting HeLa cells with a WT-microRNA mimic (green) or a ED-microRNA mimic (red), normalized to transfection of a non-targeting microRNA mimic (Ctrl microRNA). (C) Endogenous target regulation within HUAFs after transfection mediated overexpression of microRNA mimics as indicated. (B&C) Data shown represent the averages of 3 independent experiments and are presented as mean \pm SEM. * $P < 0.05$, ** $P < 0.01$, *** $P < 0.001$; by 1 sample t test versus Ctrl microRNA or 2-sided Student t test to compare WT-microRNA vs ED-microRNA treatments. (D&E) The log-fold changes (FC) of mRNA expression calculated from RNA-seq data obtained after overexpression of ED-miR-411-5p compared to overexpression of WT-miR-411-5p in HUAFs. Data represent averages of 3 independent experiments and are visualized using mean-difference plots, highlighting the predicted target genes (with a 0.5 binding score threshold to minimize false positives, see **Supplemental Table VI**) that were uniquely targeted by the WT-miR-411-5p (green, D) or ED-miR-411-5p (red, E). The overall distribution of the logFC per targetome is shown in the boxplots. Differential expression of each targetome was tested using ROAST⁶³. Target gene regulation by WT- and ED-miR-411-5p compared to a non-targeting control microRNA are shown in **Supplemental Figure VI**. (F-H) Analysis of conserved targetome expression with a predicted binding score of >0.5 (see **Supplemental Table VII**) in whole muscle tissue of C57BL/6 mice subjected to HLI using whole-genome expression data obtained via microarray²¹. Mean fold change in targetome expression of WT-, ED- or shared targets (green, red and purple respectively) of miR-376c-3p (F), miR-381-3p (G) and miR-411-5p (H) targets after HLI. Per targetome, the number of conserved targets which were detected above array background levels is indicated between brackets. Targetome expression was normalized to expression of total number of genes detected (black line) and presented as mean \pm SEM of at least 3 different mice per timepoint. * $P < 0.05$, ** $P < 0.01$; versus whole-genome expression by two-sided Student's t -test. (I&J) The combined average mRNA expression of the WT-microRNA targets (G) or ED-microRNA targets (I) validated in panels B&C within the LLV samples from 3 different patient groups (see **Figure 6**): CAD patients (LLVs without PAD, $n=8$), PAD patients (LLVs suffering severe PAD, $n=6$) and end-stage PAD patients (LLVs suffering end-stage PAD, $n=8$). Combined average expression was calculated using the average expression of individual target genes shown in **Supplemental Figure VII** and were expressed as fold change of the CAD group. Data is presented as mean \pm SEM. * $P < 0.05$, ** $P < 0.01$; by 1 sample t test.

To further validate our target predictions at a transcriptome-wide level we compared the target gene regulation after overexpression of WT- and ED-miR-411-5p using RNA-seq. MiR-411-5p was chosen because it was highly expressed in lower limb vein samples, its editing is highly conserved and we have previously shown that other isoforms of this microRNA impact the cellular response to ischemia¹⁹. We focused on the genes uniquely targeted by either WT- and ED-miR-411-5p and filtered the predicted target genes based using a binding score similar or better than those of the targets that were confirmed with other *in vitro* assays (i.e. a binding score >0.5) as threshold value to minimize the inclusion of false positive putative targets^{14,16,20}. The number of predicted targets detected in the RNA-seq dataset are summarized in **Supplemental Table VI**.

Consistent with our previous findings regarding target regulation, we found that overexpression of WT-miR-411-5p specifically lead to a global downregulation of the WT-targetome compared to a non-targeting control microRNA, while ED-miR-411-5p specifically downregulated the ED-targetome (**Supplemental Figure VI**). A direct comparison between ED- and WT-miR-411-5p overexpression showed that the ED-miR-411-5p specifically decreases the ED-targetome, while alleviating the repression of the WT-targetome relative to WT-miR-411-5p overexpression (**Figure 7D&E**).

In vivo target regulation

To examine target regulation *in vivo* after ischemia, we used whole genome expression data obtained via microarray in whole muscle tissue of C57BL/6 mice subjected to hindlimb ischemia²¹. For this analysis, we took the human WT- and ED-targetomes of miR-376c-3p, miR-381-3p and miR-411-5p (but not of miR-376a-3p due to lack of editing-conservation). First, we determined which predicted human targets are conserved as predicted targets in mice. Next, we also filtered these predictions using a binding score threshold of 0.5 to minimize the inclusion of false positive putative targets^{14,16,20}. The number of conserved predicted targets, as well as the fraction of predicted targets detected in the microarray dataset are summarized in **Supp. Table VII**.

The average expression of all three ED-microRNAs' targetomes were downregulated significantly 1 day after induction of ischemia (**Figure 7F-H**). In contrast, the WT-microRNAs' targetomes were not downregulated at any time-point.

Genes that are potentially targeted by both the ED-microRNAs and WT-microRNAs were also downregulated at both 1 and 3 days after induction hindlimb ischemia.

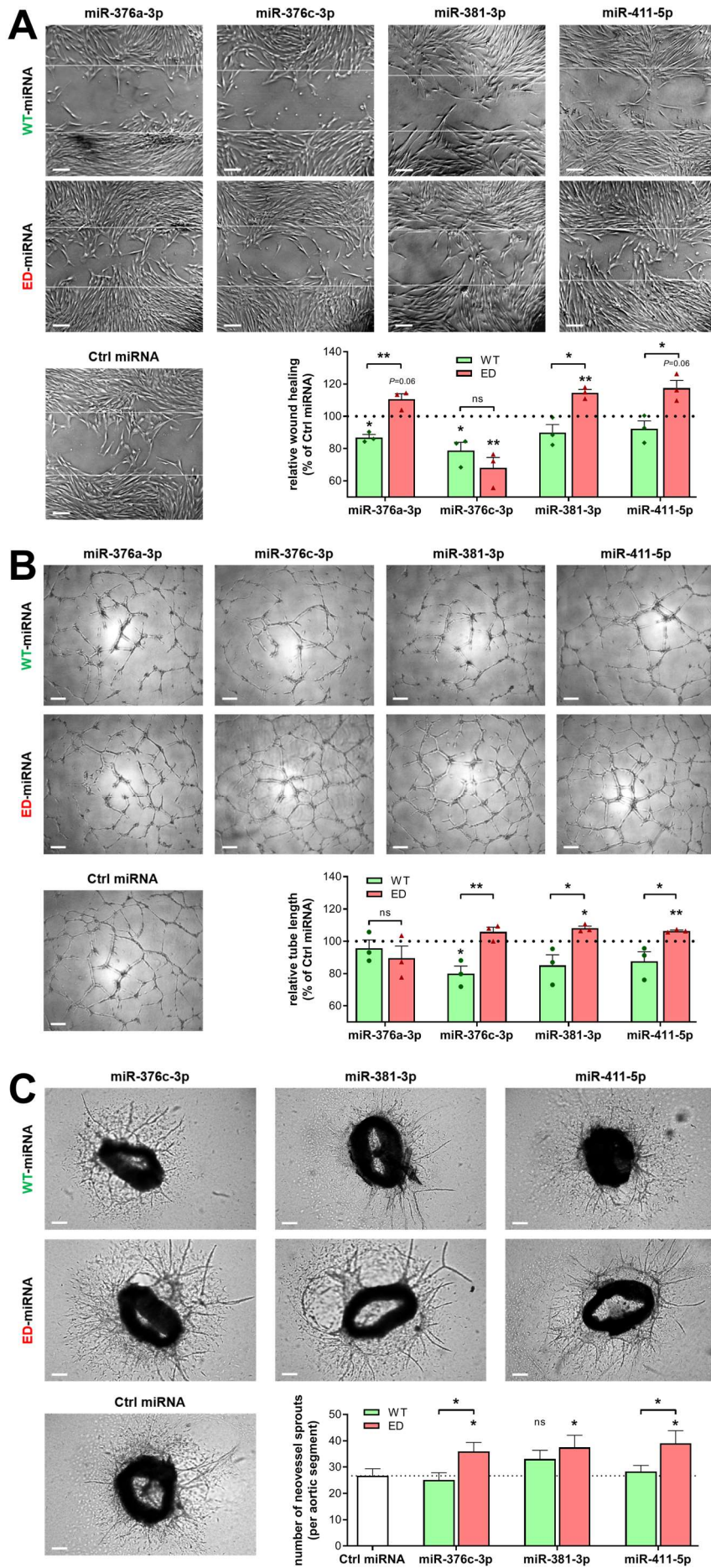
Next we examined if the human targets that we validated (see **Figure 7B&C**) were indeed regulated in the ischemic LLV samples from patients with PAD compared to the normoxic LLVs from patients with CAD. Targets of WT-microRNAs were not downregulated in the veins from patients with either PAD or end-stage PAD (**Supplemental Figure VII-A**). In contrast, ED-microRNA targets BCL2, BMP2, CHD2 and FGF2 showed decreased expression in veins from all PAD patients, compared to CAD patients (**Supplemental Figure VII-B**). A fifth ED-microRNA target, WNT4, was not expressed in these human LLVs. When combined into a single set of targets, the expression of the ED-microRNA targets was decreased significantly in both intermittent PAD patients ($P=0.001$) and end-stage PAD patients ($P=0.03$, **Figure 7J**), whereas the expression of the WT-microRNA target set was not regulated (**Figure 7I**).

Functional effects of microRNA editing

Finally, the functional implications of the observed A-to-I editing events were examined using overexpression of either the WT-microRNA or ED-microRNA in three different functional assays. First we performed scratch-wound healing assays in HUAFs. We validated that transfection-mediated microRNA-overexpression results in the desired changes in percentage microRNA editing (**Supplemental Figure V A-D**). Overexpression of all four WT-microRNAs reduced scratch-wound healing compared to the control. Treatment with ED-miR-376c-3p resulted in a comparable reduction in scratch-wound healing as WT-miR-376c-3p. However, treatment with ED-miR-376a-3p, ED-miR-381-3p and ED-miR-411-5p resulted in increased scratch-wound healing compared to the control and to their WT-microRNA counterparts (**Figure 8A**).

Next we studied the functional effects of ED-microRNAs in HUVECs by examining tube formation on Matrigel. We observed that overexpression of ED-miR-376c-3p, ED-miR-381-3p and ED-miR-411-5p induced more HUVEC tube formation than their WT-microRNA counterparts (**Figure 8B**).

Finally we studied the effects of microRNA editing on complex neovessel growth by culturing murine aortic segments *ex vivo*. We found that, compared to control microRNA-mimic treatment, overexpression of ED-miR-376c-3p, ED-miR-381-3p and



◀ **Figure 8: Functional effect of WT-microRNAs and ED-microRNAs on *in vitro* and *ex vivo* angiogenesis.** (A) Representative images and quantification of scratch-wound healing after overexpression of a WT-microRNA mimic or ED-microRNA mimic in HUAFs relative to a non-targeting microRNA mimic (Ctrl microRNA). White lines indicate original scratch wound area. (B) Representative images and quantification of HUVEC tube formation after similar treatment with microRNA mimics as indicated. (A&B) Data is presented as mean \pm SEM from 3 independent experiments performed with pooled cells from a total of 13 different umbilical cords. * $P < 0.05$, ** $P < 0.01$; by 1 sample *t* test versus Ctrl microRNA or 2-sided Student *t* test to compare WT-microRNA vs ED-microRNA treatments. (C) Representative pictures and quantification of neovessel sprouting from aortic ring segments treated with microRNA mimics as indicated. Data is presented as mean \pm SEM of at least 30 aortic segments per treatment, originating from 11 different mice. * $P < 0.05$; versus control condition unless otherwise indicated by 2-sided Student *t* test. Scale bars are 200 μ m.

ED-miR-411-5p induces the outgrowth of neovessel sprouts, while their WT-microRNA counterparts do not (Figure 8C).

Taken together, these three experimental setups demonstrate that ischemia-induced editing of vascular microRNAs enhances their angiogenic potential.

DISCUSSION

In this study, we demonstrate that post-ischemic induction of pri-microRNA A-to-I editing is a widespread phenomenon in vascular cells, occurring in at least 10 vasoactive microRNAs (including miR-487b-3p)¹⁴. MicroRNA editing appears relatively pervasive in the vasculature, as pri-microRNA A-to-I editing was found in 29% of the 35 vasoactive microRNAs that we identified as editable in a context-dependent manner. For the 4 most prevalent microRNAs, miR-376a-3p, miR-376c-3p, miR-381-3p and miR-411-5p, we demonstrate that induction of pri-microRNA editing by mimicking ischemic conditions also results in a significant increase in functional edited mature microRNAs (ED-microRNAs). The expression of these microRNAs was also increased after hindlimb ischemia *in vivo* and in veins from PAD patients. Strikingly, all the A-to-I editing events that we identified, were located in the seed-sequence of the microRNAs. We validated that seed-sequence editing indeed causes a shift in target regulation for each of the four most prevalent microRNAs, leading to pro-angiogenic functional changes in *in vitro* and *ex vivo* assays.

Our study shows an unprecedented number of microRNA editing events that are actively regulated in response to a pathological stimulus. Moreover, the newfound

edited vascular microRNAs have a significantly higher percentage editing at both baseline and under ischemic conditions compared to our initial discovery of ischemia-induced editing of miR-487b-3p. A study by Nigita *et al.* examined microRNA editing after hypoxia, albeit using a breast adenocarcinoma cell line and RNA-seq instead²². However, the authors could not establish unidirectional regulation of microRNA editing or expression. In fact, they found only 5 microRNAs that displayed A-to-I editing at low percentages, and none of these were microRNAs that we identified as edited in vascular cells. A probable explanation for the differences in microRNA editing is the tissue- and context-specificity of A-to-I editing⁷. This hypothesis is supported by the differences in microRNA expression and A-to-I editing that we found between different human organs, vascular cell types and vessels (**Figures 1, 3 and 5** respectively). Additionally, studies have shown that microRNA A-to-I editing is generally reduced in human cancer tissues, which could explain the low editing observed in the human cancer cell line^{23,24}.

We observed that expression of both ED-pri-microRNAs and mature ED-microRNAs is consistently increased in cells cultured under hypoxia+starvation to mimic ischemic conditions. However, the increase in percentage pri-microRNA editing did not always result in a similar increase in percentage mature microRNA editing, like for miR-411-5p. Similarly, a previous study also observed differences between pri-miR-411-5p and mature miR-411-5p editing in human brains²⁵. These differences in editing rates support the principle that pri-microRNA editing can affect microRNA processing dynamics, resulting in a reduced processing efficiency compared to the unedited microRNA^{11,26,27}.

A-to-I editing is directed by the enzymes ADAR1 and ADAR2. In the present study we showed that ischemia-induced vasoactive microRNA editing was consistently paired with increased expression of both ADARs *in vitro* and *in vivo*. ADAR1 and ADAR2 are also known to play editing-independent roles in microRNA biogenesis and maturation however²⁸⁻³⁰. We found that this was indeed the case for all the examined microRNAs, as repression of either ADAR1 or ADAR2 also resulted in reduced expression of both WT and ED mature microRNAs. Additionally, knockdown of ADARs also resulted in reduced expression of the pri-microRNAs. Since these primary microRNAs were formed from spliced out introns or intergenic transcripts which are usually degraded³¹, our data

suggest that ADARs may help preserve such pri-microRNA-containing transcripts and facilitate microRNA biogenesis.

However, where processing was influenced by both ADARs equally, editing of specific microRNAs was regulated by either ADAR1 or ADAR2 specifically. With the exception of pri-miR-376a1&2, and the previously reported pri-miR-487b¹⁴, all vascular pri-microRNA editing depended solely on ADAR1. For pri-miR-376a2 and pri-miR-381-3p editing, these findings were in accordance with previous ADAR perturbation experiments on human cancer cell lines^{27,32}. For the rest of the vasoactive pri-microRNA editing, our results provide the first clear validation of their dependency on ADAR1 in human cells. Editing of pri-miR-376a2 was exclusively ADAR2-dependent. Pri-miR-376a1 editing on the other hand depends both on ADAR1 and ADAR2, similar to what we previously showed for editing of pri-miR-487b-3p¹⁴. The mechanisms behind the selectivity of A-to-I editing of pri-microRNAs remain unclear as ADAR1 and ADAR2 edit distinct sets of microRNAs without a strict target sequence specificity^{8,33,34}. Nevertheless, microRNA editing events are often strongly conserved, in contrast to editing events of other RNA species in the human transcriptome^{24,35}. Many of the microRNA-editing events that we observed are conserved across species, including miR-381-3p, miR-411-5p and the miR-376 family, suggesting their biological importance^{13,24}.

Indeed, all the editing sites that we identified were located within the seed-sequence of the microRNAs. Therefore, these editing events could all lead to a novel microRNA, the ED-microRNA, which inhibits a completely different set of target mRNAs. The seed-sequence of each of the microRNAs that we found to be edited is different from any validated microRNA¹⁶. This confirms that each of these A-to-I editing events produces an entirely new microRNA with a novel targetome. Through luciferase reporter gene assays and validation of endogenous targets we showed that seed-sequence editing of miR-376a-3p, miR-376c-3p, miR-381-3p and miR-411-5p indeed completely shifts its target site selection (**Figure 7**). Finally, we demonstrated the relevance of ED-microRNAs *in vivo*, by showing that the increased expression of the edited microRNAs in mouse muscles goes hand-in-hand with a decreased expression of ED-microRNA targets but not of WT-microRNA targets.

Interestingly, pathway enrichment analyses of the putative targetomes revealed that each microRNA editing event altered enrichment for Cadherin signaling genes and, for 3 of the 4 microRNAs, also for Wnt signaling genes. Cadherins are known to play an important role in vascular cell function and angiogenesis, while Wnt signaling has been implicated to promote vascular remodeling and even cardiovascular regeneration^{36,37}. Using three different functional assays we confirmed that editing induced targetome changes result in angiogenesis-associated functional changes. We assessed the effect of WT-microRNAs and ED-microRNAs on *in vitro* scratch-wound healing and tube formation, and *ex vivo* neovessel sprouting, and consistently found that ED-microRNAs had increased pro-angiogenic properties compared to the WT-microRNAs. These results are in line with the effects of editing of miR-487b-3p, which also enhanced *in vitro* and *ex vivo* angiogenesis¹⁴.

A technical limitation to current microRNA-editing studies is the fact that it is yet not possible to manipulate microRNA-editing in vascular tissues specifically *in vivo* without also affecting the WT-microRNA expression or without large-scale off-target effects. An alternative *in vivo* experimental setup could be to quantify vascular ingrowth into subcutaneously injected matrigel plugs mixed with synthetic microRNAs. However, the potential clinical relevance of microRNA-editing has already been demonstrated in the field of oncology. MiR-378a-3p editing was shown to prevent melanoma progression via regulation of PARVA expression³⁸ and miR-455 editing was shown repress melanoma growth and reduce metastasis³⁹. Furthermore, Franzén *et al.* found that specific editing events can sometimes be associated with phenotypic traits¹² and Stellos *et al.* demonstrated the importance of A-to-I editing of the Cathepsin S mRNA in cardiovascular disease⁴⁰. We provide new evidence here that microRNA editing can play a direct role in cardiovascular disease. We demonstrate that vasoactive mature microRNAs are also edited *in vivo* in response to ischemia in a murine hindlimb ischemia model and in *ex vivo* cultured human arteries and veins. Furthermore, we found that mature microRNA editing is significantly increased in limb veins from patients with PAD, compared to limb veins from patients with CAD (**Figure 6**). These results suggest that increased microRNA editing is clinically associated with PAD.

Our unbiased screening for editable microRNAs resulted in a striking enrichment for microRNAs from the 14q32 microRNA gene cluster. Indeed of the 10 pri-microRNAs

that we confirmed to be edited, 8 microRNAs originate from this single gene cluster, including the four highest expressed microRNAs, miR-376a-3p, miR-376c-3p, miR-381-3p and miR-411-5p. MiR-487b-3p, which we previously reported to be edited, is also transcribed from the 14q32 locus. The 14q32 locus (12F1 in mice) encodes >50 microRNA genes and we, and others, have previously shown that 14q32 microRNAs, as well as the other types of noncoding RNAs from this locus, play a vital regulatory role in many aspects of cardiovascular physiology and pathology^{4,14,41-46}. Additionally, 14q32 microRNAs have been implicated in rapid placental growth during gestation by regulating capillary formation of the placenta's labyrinth zone, which fits with the microRNAs' regulatory roles in angiogenesis during adulthood⁴⁷. We now show that A-to-I editing of 14q32 microRNAs also contributes to the regulatory role of this locus in vascular remodeling.

In conclusion, we found widespread A-to-I editing of the seed-sequence of multiple vasoactive microRNAs, resulting in novel mature microRNAs. Expression of each ED-microRNA was significantly increased after ischemia and microRNA editing was also induced in ischemic veins from patients. Editing of miR-376a-3p, miR-376c-3p, miR-381-3p and miR-411-5p causes a complete shift in the targetome of the microRNA. The ED-microRNAs were functionally different from the WT-microRNAs and all ED-microRNAs enhanced certain angiogenic properties, compared to their wildtype counterparts. This study underlines the relevance of microRNA-editing in the response to ischemia. Since the editing events identified here represent only a small subset of the total pri-microRNA editing events¹⁰, future studies are likely to uncover many more editing events relevant to cardiovascular disease.

MATERIALS AND METHODS

Identification of vasoactive microRNAs containing A-to-I editable adenosines

To identify vasoactive microRNAs containing adenosines which can be subject to A-to-I editing in a context specific manner we combined manual literature curation with reanalysis of public microRNA-seq datasets.

We first searched the Pubmed database for studies that identified microRNA editing events by analyzing high throughput small RNA sequencing datasets by searching for the search terms 'microRNA' and 'A-to-I OR inosine' in the titles and

abstracts (performed December 2017). A total of 8 studies were identified that fulfilled these criteria and none were excluded^{10,23,32,48-52}. On average, these studies identified approximately 40 mature microRNAs with statistically significant A-to-I editing events. To ensure microRNA candidates are confidently edited we only included editing events that were identified in at least two different studies and/or were previously shown to be ADAR-dependent. When selecting microRNA candidates, no restrictions were applied to magnitude or tissue specificity of the editing to prevent excluding context-dependent editing events. This yielded a total of 60 confidently editable microRNAs (**Supplemental Table I**).

Next, the subset of 'vasoactive' editable microRNAs were identified by selecting microRNAs which were linked to vascular biology in previous studies. This was done by searching the microRNAs in the Pubmed database combined with the search term 'cardiovascular OR vascular OR vessel OR endothelial OR angiogenesis' (within title and abstract). MicroRNAs were considered vasoactive if at least one search result indicated that the microRNA was involved in or associated with cardiovascular function or disease (**Supplemental Table I**).

Finally, high quality public microRNA deep sequencing datasets were reanalyzed using the 'miR-seq browser' function of the miRGator webtool (mirgator.kobic.re.kr)⁵³ to examine baseline prevalence and tissue specificity of selected microRNA editing in major human organs. The datasets used were the ones with highest read counts available: GSM548639 (whole brain), SRX050631 (heart), SRX050632 (lung), SRX050633 (thymus), SRX050634 (ovary), SRX050635 (testes), SRX050636 (spleen), SRX050637 (kidney), SRX050638 (liver) and GSM494810 (PBMCs). Percentage inferred editing was calculated per editable adenosine by dividing total number of reads containing a G mismatch in that position divided by the sum of the reads with an A or a G in that position. In both cases, 3' templated isomiR reads were included since this does not alter the seed region and thus targets the same genes. MiR-376a1-3p, miR-376a2-3p and miR-376b-3p editing could not be accurately calculated separately due to their near-complete sequence homology, and was therefore expressed as percentage editing of miR-376a+b-3p.

The identification procedure of vasoactive microRNAs containing A-to-I editable adenosines is schematically summarized in **Supplemental Figure VIII**.

Isolation of primary vascular cells from human umbilical cords

Isolation and culturing of primary vascular human cells was performed as described previously¹⁴.

In brief, umbilical cords were collected from full-term pregnancies and used for either human umbilical arterial fibroblasts (HUAF) or human umbilical venous endothelial cells (HUVEC) isolation.

For HUAF isolation, the tunica adventitia was removed from the umbilical artery and incubated overnight in serum rich medium (DMEM GlutaMAX™ (Invitrogen, GIBCO, Auckland, New Zealand), 10% heat inactivated fetal bovine serum (PAA, Pasching, Austria), 10% heat inactivated human serum, 100U penicillin & 100µg streptomycin per mL (Lonza, Basel, Switzerland) and nonessential amino acids (GIBCO #11140050)). The next day the adventitia was incubated in a 2mg/ml collagenase type II solution (Worthington, Lakewood, NJ, USA) at 37 °C. The resulting cell suspension was filtered over a 70µm cell strainer, pelleted and resuspended and plated in HUAF culture medium (DMEM GlutaMAX™ (Invitrogen), 10% heat inactivated fetal bovine serum (PAA) and 100U penicillin & 100µg streptomycin per mL (Lonza)).

HUVECs were isolated from the umbilical veins by infusing a flushed vein with 0.75 mg/ml collagenase type II (Worthington) and incubated at 37°C for 20 minutes. The cell suspension was collected and pelleted and resuspended in HUVEC culture medium (M199 (PAA), 10% heat inactivated human serum (PAA), 10% heat inactivated newborn calf serum (PAA), 100U penicillin & 100µg streptomycin per mL (Lonza), 150µg/ml endothelial cell growth factor (kindly provided by Dr. Koolwijk, VU Medical Center, Amsterdam, The Netherlands) and 5U/ml heparin (LEO Pharma, Ballerup, Denmark)). HUVECs were cultured in plates coated with 10µg/ml fibronectin (Sigma-Aldrich, Steinheim, Germany).

Cell culture

Cells were cultured at 37°C in a humidified 5% CO₂ environment. Culture medium was refreshed every 2-3 days. Cells were passed using trypsin-EDTA (Sigma-Aldrich) at 70-80% confluency (HUAFs) or 90-100% (HUVECs). HUAFs were used up to passage five and HUVECs up to passage three. Stock solutions of isolated HUAFs and HUVECs

up to passage two were stored at -180°C in DMEM GlutaMAX™ containing 20% FBS and 10% DMSO (Sigma-Aldrich). Experiments were performed with pooled cells isolated from 13 different donors.

In vitro acute ischemia model

For *in vitro* ischemia experiments, HUAFs and HUVECs were seeded in separate 12 well plates at 70.000 or 100.000 cell per well, respectively. After 24h, medium was removed and cells were subjected to either control conditions (normal culture medium and ~20% oxygen) or by mimicking ischemic conditions for an additional 24h. Ischemic conditions were mimicked by culturing cells in starvation medium and hypoxia (1% oxygen). HUAF starvation medium consisted of DMEM GlutaMAX™ (Invitrogen) with 0.1% heat inactivated fetal bovine serum (PAA) and 100U penicillin & 100µg streptomycin per mL (Lonza). HUVEC starvation medium consisted of M199 (PAA), 10% heat inactivated newborn calf serum (PAA) and 100U penicillin & 100µg streptomycin per mL (Lonza). At the end of the experiment, cells were washed with PBS and harvested with TRIzol Reagent (Invitrogen).

RNA isolation and cDNA synthesis

Total RNA was isolated with TRIzol (Invitrogen), according to the manufacturer's instructions. RNA concentration and purity were examined by nanodrop (Nanodrop Technologies, Wilmington, DE, USA). For pri-miRNA experiments, DNase treatment was performed using RQ1 RNase-Free DNase (Promega, Madison, WI, USA) according to manufacturer's instructions. Total complementary DNA (cDNA) was prepared using the High Capacity cDNA Reverse Transcription Kit (Applied Biosystems, Foster City, CA, USA) according to manufacturer's protocol.

Quantification of primary microRNA editing by Sanger sequencing

Primary microRNAs (pri-miRNA) sequencing was performed as previously described¹⁴. Genomic DNA (gDNA) was isolated from the interphase according to TRIzol Reagent instructions to ensure observed cDNA sequencing variation was not due to SNPs. The pri-miRNA of each selected 'editable' microRNA was individually amplified by polymerase chain reaction (PCR) from HUAF gDNA and cDNA samples with GoTaq DNA Polymerase (Promega) or HotStarTaq DNA Polymerase (QIAGEN,

Hilden, Germany) (for primer sequences, see **Supplemental Table VIII**). Gel electrophoresis of the product was performed after which the correctly sized DNA band was excised and purified using Wizard SV Gel and PCR Clean-Up System (Promega). Amplified and purified pri-miRNA samples were submitted for Sanger sequencing to the Leiden Genome Technology Center (Leiden, The Netherlands) according to their instructions.

A-to-I editing presents itself as A-to-G substitutions on the resulting sequencing chromatograms. Therefore, the location of each genomic adenosine was analyzed for presence of a secondary guanosine peak in the chromatogram from the cDNA samples. gDNA sequencing chromatograms were used to ensure A-to-G substitutions were cDNA specific. Percentage pri-miRNA A-to-I editing was calculated as described previously⁵⁴. In summary, editing is equal to the height of the editing peak (the secondary G peak) expressed as a percentage of the combined heights of the overlapping A and G peaks.

Quantification of pri-miRNA and mRNA expression

The expression of pri-miRNAs and mRNAs within cDNA samples was quantified by qPCR using Quantitect SYBR Green (QIAGEN) on the ViiA7 Real-Time PCR System (Applied Biosystems). Pri-miRNA expression was normalized against the stably expressed non-coding RNA U6. Pri-miRNA expression was combined with percentage editing to calculate individual expression of WT- and ED-pri-miRNA. mRNA expression was measured with intron-spanning primers and normalized against RPLP0 mRNA expression, a household gene that remains stable under ischemic conditions⁴⁰. All primer sequences are provided in **Supplemental Table VIII**.

ADAR1 and ADAR2 protein quantification by Western blot

Protein was isolated from cell and human LLV lysates with TRIzol (Invitrogen), according to the manufacturer's instructions. Total protein concentration was quantified by Pierce BCA Protein Assay Kit (ThermoFisher Scientific, Waltham, MA, USA) after which protein concentration was normalized to 1µg/µL in Laemmli buffer (Bio-Rad Laboratories, Hercules, CA, USA) containing 10% β-mercaptoethanol (Sigma-Aldrich).

Samples were heated to 95°C for 5 minutes and cooled before loading 1 µg of protein per lane in a 4–15% Mini-PROTEAN TGM Precast Protein Gel (Bio-Rad Laboratories). Protein separation was performed in Vertical Electrophoresis Cell using premixed Tris/glycine/SDS running buffer (both Bio-Rad Laboratories). Proteins were transferred onto a nitrocellulose membrane (GE Healthcare Life Sciences, Eindhoven, The Netherlands) by a wet transfer using premixed Tris/glycine transfer buffer (Bio-Rad Laboratories). The membrane was blocked at room temperature in 5% non-fat dried milk in TBS-T (150mM NaCl; 50mM Tris; 0,05% Tween-20 (Sigma-Aldrich)) and subsequently incubated overnight at 4°C with antibodies against ADAR1 (Abcam ab168809, 1:500 dilution), ADAR2 (Abcam ab64830, 1:500 dilution) or stable household protein beta actin (Abcam ab8226, 1:1000 dilution), diluted in 5% non-fat dried milk in TBS-T. After multiples washes with TBS-T, the membrane was incubated at room temperature with anti-rabbit peroxidase conjugated secondary antibody (31462, ThermoFisher Scientific), diluted to 1:10000 in 5% non-fat dried milk in TBS-T. Proteins of interest were revealed using SuperSignal™ West Pico PLUS Chemiluminescent Substrate (ThermoFisher Scientific) and imaged using the ChemiDoc Touch Imaging System (Bio-Rad Laboratories). ADAR1 and ADAR2 expression was quantified relative to stable household protein beta actin using ImageJ.

Quantification of mature microRNA expression and editing

Specific quantification of unedited ‘wildtype’ microRNA (WT-miRNA) expression and edited microRNA (ED-miRNA) expression was performed using TaqMan qRT-PCR microRNA assays designed by and purchased from Applied Biosystems. WT-miRNA assays were predesigned while ED-miRNA assays were custom designed TaqMan Small RNA assay specifically targeting the edited sequence where the inosine was replaced by a guanosine instead. Oligo sequences used for each custom ED-miRNA specific qRT-PCR assay are presented in **Supplemental Table IX**.

Expression quantification was performed according to manufacturer’s instructions. Briefly, RNA was reverse transcribed into microRNA-specific cDNA using the Taqman MicroRNA Reverse Transcription Kit (Applied Biosystems). Samples were run in triplicate on a ViiA7 (Applied Biosystems). Relative expression of WT-miRNA and ED-miRNAs was calculated relative to noncoding household RNA U6. Amplification

efficiency of all qRT-PCR kits was characterized using serial dilution (**Supplemental Figure II B-E**) and incorporated in expression calculations. Percentage microRNA editing was calculated per mature microRNA by expressing ED-miRNA as a percentage of the combined expression of both WT- and ED-miRNA.

AGO2 immunoprecipitation and quantification of associated miRNAs

RNA binding protein immunoprecipitation (RIP) was performed using the EZMagna RIP kit (Millipore). HUAF cells were seeded in T75 flasks. After 24h, medium was removed and cells were subjected to either control conditions (normal culture medium and ~20% oxygen) or hypoxia+starvation conditions for an additional 24h. Cells were then washed with cold PBS, trypsinized and pelleted at 300g using a table-top centrifuge. The cell pellet was then resuspended in 0.4% formaldehyde to crosslink of RNA-protein complexes for 30 min on ice. Next, cells were pelleted and washed twice with cold PBS, after which the cell pellet was resuspended in complete RIP lysis buffer. Per RIP reaction, HUAF lysate from 2 T75 culture flasks were incubated with RIP buffer containing magnetic beads conjugated with antibodies against AGO2 (Abcam ab32381) and negative control rabbit control IgG (Millipore PP64B). After completing the RIP according to the manufacturer's protocol, the samples were treated with proteinase K to digest protein and RNA was isolated using TRIzol LS reagent (Invitrogen).

cDNA was made as described above. Finally, the expression of mature WT-miRNAs and ED-miRNAs in each RIP fraction was measured as described above, to determine if these microRNAs are indeed associated with AGO2 and if hypoxia+starvation conditions also affects the amount of microRNA associated with AGO2.

siRNA mediated knockdown of ADAR1 and ADAR2

Knockdown of ADAR1 and ADAR2 in HUAFs was performed as previously described¹⁴. Briefly, HUAFs were seeded in 12 well plates, grown to 70% confluence and then transfected using Lipofectamine RNAiMAX (Invitrogen) according to the manufacturer's protocol, with a final concentration of 27.5 nM siRNA. siRNA sequences used were originally reported and validated by Stellos *et al.*⁴⁰ and can be found in **Supplemental Table X**. After 48 hours, cells were washed 3 times with PBS

and total RNA was isolated and cDNA was synthesized as before. Expression of *ADARI*, *ADAR2* and *RPLP0* was quantified to determine knockdown efficiency. Subsequent microRNA expression and editing analyses were performed as described above.

Hindlimb Ischemia Model

All animal experiments were approved by the committee on animal welfare of the Leiden University Medical Center (Leiden, The Netherlands, approval reference number 09163).

Adult male C57Bl/6 mice, 8 to 12 weeks old (Charles River, Wilmington, MA, USA) were housed in groups of 3 to 5 animals, with free access to tap water and regular chow. The assignment of the mice to the experimental groups was conducted randomly. All animals were included in the study and the definition of inclusion and exclusion criteria as well as primary and secondary endpoints was not applicable.

Induction of HLI was performed as described previously¹⁴. In brief, mice were anesthetized by intraperitoneal injection of midazolam (5 mg/kg, Roche Diagnostics, Almere, The Netherlands), medetomidine (0.5 mg/kg, Orion, Espoo, Finland) and fentanyl (0.05 mg/kg, Janssen Pharmaceuticals, Beerse, Belgium). Unilateral HLI was induced by electrocoagulation of the left femoral artery proximal to the superficial epigastric arteries. After surgery, anesthesia was antagonized with flumazenil (0.5 mg/kg, Fresenius Kabi, Bad Homburg vor der Höhe, Germany), atipamezole (2.5 mg/kg, Orion) and buprenorphine (0.1 mg/kg, MSD Animal Health, Boxmeer, The Netherlands). Mice were sacrificed by cervical dislocation and the adductor and gastrocnemius muscles were excised en bloc and snap-frozen on dry ice before (T0) and at 1 and 3 days (T1 and T3 respectively) after induction of HLI. Muscle tissues were crushed with pestle and mortar, while using liquid nitrogen to preserve sample integrity. Tissue homogenates were stored at -80°C. Total RNA was isolated from tissue powder by standard TRIzol-chloroform extraction as before.

Collection of surplus human artery and vein samples

All human artery and vein samples were collected at the Leiden University Medical Center. Collection, storage, and processing of the samples were performed in compliance with the Medical Treatment Contracts Act (WGBO, 1995) and the Code of Conduct for Health Research using Body Material (Good Practice Code, Dutch

Federation of Biomedical Scientific Societies, 2002) and the Dutch Personal Data Protection Act (WBP, 2001).

Human vena saphena magna (VSM) and internal mammary arteries (IMA) were harvested during elective coronary bypass surgery on patients with coronary artery disease. Only surplus tissue was collected. These samples were anonymized and no data were recorded that could potentially trace back to an individual's identity. Vessels were left to rest overnight in culture medium (DMEM Glutamax with 10% heat inactivated fetal calf serum and 100U penicillin & 100µg streptomycin per mL) at 37°C and 20% oxygen and subsequently cultured for 24h, either at control conditions (20% oxygen and culture medium) or at hypoxia+starvation conditions (1% oxygen and fetal calf serum reduced to 0.5%). VSMs were left intact and snap frozen directly. Before snap freezing the IMAs, they were separated manually into the tunica adventitia and the tunica media/intima, while kept cold. Frozen tissues were crushed in liquid nitrogen and total RNA was isolated from tissue powder by standard TRIzol-chloroform extraction as described above.

Surplus lower limb vein (LLV) tissue samples were also collected during coronary bypass-surgery and femoral artery to popliteal artery-bypass surgery.

LLVs from 8 patients with end-stage PAD were obtained directly after lower limb amputation. Inclusion criteria for the biobank were a minimum age of 18 years and lower limb amputation, excluding ankle, foot, or toe amputations. The exclusion criteria were suspected or confirmed malignancy and inability to give informed consent. Sample collection was approved by the Medical Ethics Committee of the Leiden University Medical Center (Protocol No. P12.265) and written informed consent was obtained from these participants.

All human artery and vein samples were snap-frozen and stored at -80°C. Frozen tissues were crushed in liquid nitrogen and total RNA was isolated from tissue powder by standard TRIzol-chloroform extraction as described above.

In silico target prediction and pathway enrichment analysis

Putative human targetomes of each microRNA were determined using three distinct target prediction algorithms to reduce the number of false positives: Targetscan (www.targetscan.org)¹⁶, miRanda (www.microRNA.org)⁵⁵ and Diana-MR-

microT (diana.imis.athena-innovation.gr)²⁰. Targetscan (version 6.2) and miRanda (2010 release) predictions were obtained through the miRmut2go webtool (compbio.uthsc.edu/miR2GO)⁵⁶ whereas Diana-MR-microT predictions were obtained using its website. In the predictions, the inosine was replaced with guanosine for the ED-miRNA input sequence. No restrictions were applied for target prediction. Genes were only considered to be a particular microRNA's putative target gene if each of the 3 target prediction algorithms identified them as a target.

For each targetome, the set of target genes of a particular microRNA, overrepresented pathways were identified using PANTHER pathway enrichment analysis (www.pantherdb.org, version II)¹⁸ as described previously⁵⁷.

To identify putative target genes involved in the response to ischemia, several relevant gene ontology terms were selected, including “response to hypoxia”, “angiogenesis” and “migration” (geneontology.org) (**Supplemental Table V**). Putative target genes exclusively targeted by either the WT or ED variant of a particular microRNA were considered involved in the response to ischemia if they were associated with one or multiple of these terms.

Dual Luciferase Reporter Gene Assays

Constructs: 3'UTR sequences containing one or more WT- or ED-miRNA binding sites from endogenous target genes were amplified from human cDNA using primers with a short extension containing cleavage sites for XhoI (5'-end) and NotI (3'-end) (**Supplemental Table VIII**). For BMP2, BCL2 and ANGPT2 (ED-miR-381-3p binding sequences only) endogenous binding sequences were purchased from IDT (Integrated DNA Technologies, Coralville, USA) instead (**Supplemental Table X**).

Amplicons and synthetic sequences were digested with XhoI and NotI and cloned in between the XhoI and NotI cleavage sites of the PsiCHECK™-2 vector (Promega) at the 3'-end of the coding region of the Renilla luciferase reporter gene. The sequence of each construct was confirmed using Sanger sequencing.

Sequences of the primers used are available in **Supplemental Table VIII**.

Luciferase Assays: HeLa cells were cultured at 37°C under 5% CO₂ using DMEM (GIBCO) with high glucose and stable L-glutamine, supplemented with 10% fetal calf serum and 100U penicillin & 100ug streptomycin per mL (Lonza). For experiments,

HeLa cells were grown to 75-80% confluence in white 96 well plates in their normal growth medium, at 37°C under 5% CO₂. Lipofectamine 3000 (Invitrogen) in Opti-MEM (GIBCO) was used, according to manufacturer's instructions, to transfect each well with 30 ng of PsiCHECK2-vector containing endogenous miRNA binding sequences or the original empty vector. Cells were co-transfected with 2 pmol miRcury LNA miRNA mimic for either a WT-miRNA, ED-miRNA or negative control miRNA (QIAGEN) at a concentration of 10 nM. Firefly- and Renilla-luciferase were measured in cell lysates using a Dual-Luciferase Reporter Assay System (Promega) according to manufacturer's protocol on a Cytation™ 5 plate reader (BioTek, Winooski, VT, USA). Firefly luciferase activity was used as an internal control for cellular density and transfection efficiency. The luminescence ratios were corrected for differences in baseline vector luminescence observed in vehicle treated group and expressed as percentage of scrambled control luminescence.

Displayed luciferase data represent the averages from three independent experiments.

Endogenous transcript regulation by WT-miRNAs or ED-miRNAs

Endogenous transcript regulation was examined by overexpression of WT-miRNA or ED-miRNA in HUAFs. HUAFs were seeded in 12 wells plates at 70.000 cells per well and grown for 12h in culture medium after which the medium was replaced with starvation medium to synchronise cell cycle. After another 12h, Lipofectamine RNAiMAX (Invitrogen) in Opti-MEM (GIBCO) was used according to manufacturer's instructions to transfect each well with 1 pg of miRcury LNA miRNA mimic for either a WT-miRNA, ED-miRNA or negative control miRNA (QIAGEN). After 12h, transfection medium was replaced with new starvation medium. After 14h (26h total after transfection), cells were washed twice with PBS and harvested with TRIzol reagent, after which RNA was isolated.

To examine target mRNA expression of individual genes, total cDNA was prepared and target mRNA expression was measured by qPCR as described above. Target mRNA expression was normalized against RPLP0. The intron spanning primers used can be found in **Supplemental Table VIII**. Displayed endogenous target regulation represent the averages from three independent experiments.

Targetome regulation by WT-miR-411-5p and ED-miR-411-5p

For each independent miR-411-5p overexpression experiment, at least 500ng of pooled total RNA was submitted to BGI Hong Kong for RNA-seq. BGI's services included mRNA enrichment and purification using Oligo dT Selection, RNA fragmentation, reverse transcription, end repair, adaptor ligation, DNA nanoball synthesis and finally sequencing on the DNBseq platform.

Raw reads were filtered by BGI Genomics to remove adapter sequences, contaminations and low-quality reads. Quality of the clean fastQ files was verified using FastQC version 0.11.8 (www.bioinformatics.babraham.ac.uk/projects/fastqc/). Reads were then mapped to the human genome using HISAT2 version 2.2.0 with the pre-compiled index GRCh38_snp_tran⁵⁸ and subsequently assembled into transcripts using StringTie version 2.1.1⁵⁹. Transcript abundance was estimated per gene using Rsubread version 2.0.1⁶⁰. Read count normalization and filtering was done using edgeR, retaining all genes that had > 1 count per million (cpm) in ≥ 3 samples⁶¹. Differential expression analysis was performed on voom transformed log₂ cpm values using limma⁶². Finally, enrichment of the predicted targetomes for WT and ED miR-411-5p was tested using ROAST, a self-contained gene set test⁶³. P-values were calculated by simulation, using 999 rotations. Data were visualized using limma's plotMD and R's built-in boxplot functions.

In vivo targetome regulation after Hindlimb Ischemia

For each human targetome, except the unconserved miR-376a-3p, target genes which were also predicted to be target genes in mice according to the murine Diana-MR-microT algorithm (diana.imis.athena-innovation.gr)²⁰ were considered the conserved murine targetome. On average, 62.5% of the human target genes were identified to be conserved targets in mice in this way (see **Supplemental Table VII**).

To assess which conserved targetomes are regulated in response to HLI, we used a previously published whole genome expression microarray dataset in which transcriptome expression was measured before and after HLI in the adductor muscle (Nossent *et al*²¹). For each gene detected above background levels (21074 out of 45200), post-ischemic expression was calculated relative to its expression before HLI

(TO) by calculating the $2^{\Delta\text{Log}2(\text{measured gene intensity})}$. Average putative targetome expression was determined by calculating the average post-ischemic change in expression of all genes within the particular targetome. Targetome expressions were compared to the average expression of all genes above detection limit.

Effects of WT-miRNAs or ED-miRNAs on in vitro scratch-wound healing

Effects of WT-miRNA or ED-miRNA overexpression on scratch-wound healing of HUAFs were examined. HUAFs were seeded and transfected as described above. Transfection medium was removed after 12h. Next, a p200 pipette tip was used to introduce a scratch-wound across the diameter of each well. Subsequently, the cells were washed with sterile PBS and medium was replaced with new serum starvation medium. Three locations along the scratch-wound were marked per well. The scratch-wound at these sites was imaged at time 0h and 14h after scratch-wound introduction using live phase-contrast microscopy (Axiovert 40C, Carl Zeiss, Oberkochen, Germany). After the 14h timepoint, cells were washed 3 times in PBS and then lysed and harvested in TRIzol for RNA isolation as before. MiRNA overexpression efficiency was validated by measuring miRNA expression as described above. For each imaged location, the area of the scratch-wound at 0h was superimposed on the 14h scratch-wound area image. Scratch wound healing was then determined per well as the newly covered scratch-wound area after 14h using the wound healing tool macro for ImageJ. Displayed scratch-wound healing represent the averages from three independent experiments.

Effects of WT-miRNAs or ED-miRNAs on HUVEC tube formation

HUVECs were seeded in 12-well plates in EBM-2 Basal medium (CC-3156, Lonza) supplemented with EGM-2 SingleQuots Supplements (CC-4176, Lonza). At 80% confluency, each well was transfected with 1 pg of miRcury LNA miRNA mimics as described before, using Lipofectamine RNAiMAX (Invitrogen) in Opti-MEM (GIBCO) according to manufacturer's instructions. After 24h, the transfected HUVECs were detached using trypsin-EDTA (Sigma, Steinheim, Germany) and counted. Next, low serum medium (EBM-2 Basal Medium (CC-3156) supplemented with 0.2% FBS and 1% GA-1000) was used to seed 15,000 cells per well in a 96-wells plate, which was pre-coated with 50 μL /well of Geltrex extracellular matrix (A1413202, Gibco). After 12

hours incubation, pictures of each well were taken using live phasecontrast microscopy (Axiovert 40C, Carl Zeiss). Total length of the tubes formed was analyzed using the Angiogenesis Analyzer plugin for ImageJ.

Effects of WT-miRNAs or ED-miRNAs on ex-vivo angiogenesis

Mouse aortic ring assays were performed as described previously^{4,64}. In brief, six thoracic aortas were removed from 8 to 10-week old mice, after which the surrounding fat and branching vessels were carefully removed and the aorta was flushed with Opti-MEM (Gibco). Aortic rings of ~1 mm were cut and the rings from each mouse aorta were divided over 7 wells of a 24 well plate groups for separate treatments. The different groups were then transfected overnight with 1 pg of miRcury LNA miRNA mimics, using 1.5 μ L Lipofectamine RNAiMAX (Invitrogen) in fresh Opti-MEM (GIBCO) with a total volume of 500 μ L.

The next day 96-well plates were coated with 75 μ l collagen matrix (Collagen (Type I, Millipore) diluted in 1x DMEM (Gibco) and pH adjusted with 5N NaOH). One aortic ring per well was embedded in the collagen matrix, for a total of at least 30 rings per pre-miRNA treatment. After letting the collagen solidify for an hour, 150 μ l Opti-MEM supplemented with 2.5% FBS (PAA, Austria), penicillin-streptomycin (PAA, Austria) and 30 ng/mL VEGF (R&D systems). Medium was refreshed every 2 days and was supplemented with microRNA mimics at a concentration of 100 nM, without transfection agent. Pictures of each embedded aortic ring and their neovessel outgrowth were made after 7 days using live phase-contrast microscopy (Axiovert 40C, Carl Zeiss). The number of neovessel sprouts were manually counted per aortic segment. Segments were excluded if they were too close to an obstacle (i.e. the wall of the well) or showed no outgrowth. Each neovessel emerging from the ring was counted as a sprout. Individual branches arising from each microvessel were counted as a separate sprout.

Statistical Analysis

All results are expressed as mean \pm SEM. Normality of data obtained was examined using the Shapiro-Wilk normality test. Since all variables measured were continuous parameters, pairwise comparisons were tested using either *t*-tests or 1-way ANOVA. *P*-values less than or equal to 0.05 were considered statistically significant.

ACKNOWLEDGEMENTS

We thank the vascular and thoracic surgeons of the LUMC that helped with collecting the patient material. Furthermore, we acknowledge D.A.L. van den Homberg, J.S.A. van der Geest, E. Kalbus and A.W. Meijer for their technical support.

Sources of funding

This study was supported by a grant from the Dutch Heart Foundation (Dr. E. Dekker Senior Postdoc, 2014T102), the LUMC Johanna Zaaijer Fund (2017) and the Austrian Science Fund FWF (Lise Meitner Grant, M 2578-B30).

Author Contributions

Conceptualization, RVCTK, AYN and PHAQ; Methodology, RVCTK, LP, MLB, FB, EHABP, MRV and AYN; Investigation, RVCTK, LP, EI and EHABP; Resources, EACG, KHS, MP and MRV; Writing – Original Draft, RVCTK; Writing – Review & Editing, RVCTK, PHAQ and AYN; Visualization, RVCTK; Supervision, RVCTK, PHAQ and AYN; Funding Acquisition, AYN.

Disclosure/Conflict of interest

None.

REFERENCES

1. Welten, SM, Goossens, EA, Quax, PH, and Nossent, AY (2016). The multifactorial nature of microRNAs in vascular remodelling. *Cardiovascular research* **110**: 6-22.
2. Ha, M, and Kim, VN (2014). Regulation of microRNA biogenesis. *Nat Rev Mol Cell Biol* **15**: 509-524.
3. Romaine, SP, Tomaszewski, M, Condorelli, G, and Samani, NJ (2015). MicroRNAs in cardiovascular disease: an introduction for clinicians. *Heart (British Cardiac Society)* **101**: 921-928.
4. Welten, SM, Bastiaansen, AJ, de Jong, RC, de Vries, MR, Peters, EA, Boonstra, MC, Sheikh, SP, La Monica, N, Kandimalla, ER, Quax, PH, *et al.* (2014). Inhibition of 14q32 MicroRNAs miR-329, miR-487b, miR-494, and miR-495 increases neovascularization and blood flow recovery after ischemia. *Circ Res* **115**: 696-708.
5. Mallela, A, and Nishikura, K (2012). A-to-I editing of protein coding and noncoding RNAs. *Critical reviews in biochemistry and molecular biology* **47**: 493-501.
6. Nigita, G, Veneziano, D, and Ferro, A (2015). A-to-I RNA Editing: Current Knowledge Sources and Computational Approaches with Special Emphasis on Non-Coding RNA Molecules. *Frontiers in Bioengineering and Biotechnology* **3**.
7. Tan, MH, Li, Q, Shanmugam, R, Piskol, R, Kohler, J, Young, AN, Liu, KI, Zhang, R, Ramaswami, G, Ariyoshi, K, *et al.* (2017). Dynamic landscape and regulation of RNA editing in mammals. *Nature* **550**: 249-254.
8. Nishikura, K (2016). A-to-I editing of coding and non-coding RNAs by ADARs. *Nat Rev Mol Cell Biol* **17**: 83-96.
9. Kawahara, Y, Megraw, M, Kreider, E, Iizasa, H, Valente, L, Hatzigeorgiou, AG, and Nishikura, K (2008). Frequency and fate of microRNA editing in human brain. *Nucleic Acids Res* **36**: 5270-5280.
10. Li, L, Song, Y, Shi, X, Liu, J, Xiong, S, Chen, W, Fu, Q, Huang, Z, Gu, N, and Zhang, R (2018). The landscape of miRNA editing in animals and its impact on miRNA biogenesis and targeting. *Genome Res* **28**: 132-143.
11. Yang, W, Chendrimada, TP, Wang, Q, Higuchi, M, Seeburg, PH, Shiekhattar, R, and Nishikura, K (2006). Modulation of microRNA processing and expression through RNA editing by ADAR deaminases. *Nat Struct Mol Biol* **13**: 13-21.
12. Franzen, O, Ermel, R, Sukhvasi, K, Jain, R, Jain, A, Betsholtz, C, Giannarelli, C, Kovacic, JC, Ruusalepp, A, Skogsberg, J, *et al.* (2018). Global analysis of A-to-I RNA editing reveals association with common disease variants. *PeerJ* **6**: e44466.
13. Kawahara, Y, Zinshteyn, B, Sethupathy, P, Iizasa, H, Hatzigeorgiou, AG, and Nishikura, K (2007). Redirection of silencing targets by adenosine-to-inosine editing of miRNAs. *Science* **315**: 1137-1140.
14. van der Kwast, RVCT, van Ingen, E, Parma, L, Peters, HAB, Quax, PHA, and Nossent, AY (2018). Adenosine-to-Inosine Editing of MicroRNA-487b Alters Target Gene Selection After Ischemia and Promotes Neovascularization. *Circ Res* **122**: 444-456.
15. Newman, AC, Nakatsu, MN, Chou, W, Gershon, PD, and Hughes, CC (2011). The requirement for fibroblasts in angiogenesis: fibroblast-derived matrix proteins are essential for endothelial cell lumen formation. *Molecular biology of the cell* **22**: 3791-3800.
16. Agarwal, V, Bell, GW, Nam, JW, and Bartel, DP (2015). Predicting effective microRNA target sites in mammalian mRNAs. *eLife* **4**.
17. Hellingman, AA, Bastiaansen, AJ, de Vries, MR, Seghers, L, Lijkwan, MA, Lowik, CW, Hamming, JF, and Quax, PH (2010). Variations in surgical procedures for hind limb ischaemia mouse models result in differences in collateral formation. *European journal of vascular and endovascular surgery : the official journal of the European Society for Vascular Surgery* **40**: 796-803.

18. Mi, H, Huang, X, Muruganujan, A, Tang, H, Mills, C, Kang, D, and Thomas, PD (2017). PANTHER version II: expanded annotation data from Gene Ontology and Reactome pathways, and data analysis tool enhancements. *Nucleic Acids Res* **45**: D183-D189.
19. van der Kwast, R, Woudenberg, T, Quax, PHA, and Nossent, AY (2019). MicroRNA-41l and Its 5'-IsomiR Have Distinct Targets and Functions and Are Differentially Regulated in the Vasculature under Ischemia. *Molecular therapy : the journal of the American Society of Gene Therapy*.
20. Paraskevopoulou, MD, Georgakilas, G, Kostoulas, N, Vlachos, IS, Vergoulis, T, Reczko, M, Filippidis, C, Dalamagas, T, and Hatzigeorgiou, AG (2013). DIANA-microT web server v5.0: service integration into miRNA functional analysis workflows. *Nucleic Acids Res* **41**: W169-173.
21. Nossent, AY, Bastiaansen, AJ, Peters, EA, de Vries, MR, Aref, Z, Welten, SM, de Jager, SC, van der Pouw Kraan, TC, and Quax, PH (2017). CCR7-CCL19/CCL21 Axis is Essential for Effective Arteriogenesis in a Murine Model of Hindlimb Ischemia. *Journal of the American Heart Association* **6**.
22. Nigita, G, Acunzo, M, Romano, G, Veneziano, D, Lagana, A, Vitiello, M, Wernicke, D, Ferro, A, and Croce, CM (2016). microRNA editing in seed region aligns with cellular changes in hypoxic conditions. *Nucleic Acids Res* **44**: 6298-6308.
23. Pinto, Y, Buchumenski, I, Levanon, EY, and Eisenberg, E (2018). Human cancer tissues exhibit reduced A-to-I editing of miRNAs coupled with elevated editing of their targets. *Nucleic Acids Res* **46**: 71-82.
24. Warnefors, M, Liechti, A, Halbert, J, Valloton, D, and Kaessmann, H (2014). Conserved microRNA editing in mammalian evolution, development and disease. *Genome Biol* **15**: R83.
25. Jepson, JE, and Reenan, RA (2008). RNA editing in regulating gene expression in the brain. *Biochimica et biophysica acta* **1779**: 459-470.
26. Tomaselli, S, Galeano, F, Alon, S, Raho, S, Galardi, S, Polito, VA, Presutti, C, Vincenti, S, Eisenberg, E, Locatelli, F, *et al.* (2015). Modulation of microRNA editing, expression and processing by ADAR2 deaminase in glioblastoma. *Genome Biol* **16**: 5.
27. Alon, S, Mor, E, Vigneault, F, Church, GM, Locatelli, F, Galeano, F, Gallo, A, Shomron, N, and Eisenberg, E (2012). Systematic identification of edited microRNAs in the human brain. *Genome Research* **22**: 1533-1540.
28. Ota, H, Sakurai, M, Gupta, R, Valente, L, Wulff, BE, Ariyoshi, K, Iizasa, H, Davuluri, RV, and Nishikura, K (2013). ADAR1 forms a complex with Dicer to promote microRNA processing and RNA-induced gene silencing. *Cell* **153**: 575-58 .
29. Qi, L, Song, Y, Chan, THM, Yang, H, Lin, CH, Tay, DJT, Hong, H, Tang, SJ, Tan, KT, Huang, XX, *et al.* (2017). An RNA editing/dsRNA binding-independent gene regulatory mechanism of ADARs and its clinical implication in cancer. *Nucleic Acids Res*.
30. Kawahara, Y, Zinshteyn, B, Chendrimada, TP, Shiekhattar, R, and Nishikura, K (2007). RNA editing of the microRNA-151 precursor blocks cleavage by the Dicer-TRBP complex. *EMBO Rep* **8**: 763-769.
31. Houseley, J, and Tollervey, D (2009). The many pathways of RNA degradation. *Cell* **136**: 763-776.
32. Wang, Y, Xu, X, Yu, S, Jeong, KJ, Zhou, Z, Han, L, Tsang, YH, Li, J, Chen, H, Mangala, LS, *et al.* (2017). Systematic characterization of A-to-I RNA editing hotspots in microRNAs across human cancers. *Genome Res* **27**: 1112-1125.
33. Nishikura, K (2010). Functions and regulation of RNA editing by ADAR deaminases. *Annu Rev Biochem* **79**: 321-349.
34. Bass, BL (2002). RNA editing by adenosine deaminases that act on RNA. *Annu Rev Biochem* **71**: 817-846.
35. Pinto, Y, Cohen, HY, and Levanon, EY (2014). Mammalian conserved ADAR targets comprise only a small fragment of the human editosome. *Genome Biol* **15**: R5.

36. Hermans, KC, and Blankesteyn, WM (2015). Wnt Signaling in Cardiac Disease. *Comprehensive Physiology* **5**: 1183-1209.
37. Blaise, S, Polena, H, and Vilgrain, I (2015). Soluble vascular endothelial-cadherin and auto-antibodies to human vascular endothelial-cadherin in human diseases: Two new biomarkers of endothelial dysfunction. *Vasc Med* **20**: 557-565.
38. Velazquez-Torres, G, Shoshan, E, Ivan, C, Huang, L, Fuentes-Mattei, E, Paret, H, Kim, SJ, Rodriguez-Aguayo, C, Xie, V, Brooks, D, *et al.* (2018). A-to-I miR-378a-3p editing can prevent melanoma progression via regulation of PARVA expression. *Nat Commun* **9**: 461.
39. Shoshan, E, Mobley, AK, Braeuer, RR, Kamiya, T, Huang, L, Vasquez, ME, Salameh, A, Lee, HJ, Kim, SJ, Ivan, C, *et al.* (2015). Reduced adenosine-to-inosine miR-455-5p editing promotes melanoma growth and metastasis. *Nat Cell Bio* **17**: 311-321.
40. Stellos, K, Gatsiou, A, Stamatelopoulos, K, Perisic Matic, L, John, D, Lunella, FF, Jae, N, Rossbach, O, Amrhein, C, Sigala, F, *et al.* (2016). Adenosine-to-inosine RNA editing controls cathepsin S expression in atherosclerosis by enabling HuR-mediated post-transcriptional regulation. *Nat Med* **22**: 1140-1150.
41. Nossent, AY, Eskildsen, TV, Andersen, LB, Bie, P, Bronnum, H, Schneider, M, Andersen, DC, Welten, SM, Jeppesen, PL, Hamming, JF, *et al.* (2013). The 14q32 microRNA-487b targets the antiapoptotic insulin receptor substrate 1 in hypertension-induced remodeling of the aorta. *Ann Surg* **258**: 743-751.
42. Wezel, A, Welten, SM, Razawy, W, Lagrauw, HM, de Vries, MR, Goossens, EA, Boonstra, MC, Hamming, JF, Kandimalla, ER, Kuiper, J, *et al.* (2015). Inhibition of MicroRNA-494 Reduces Carotid Artery Atherosclerotic Lesion Development and Increases Plaque Stability. *Ann Surg* **262**: 841-847; discussion 847-848.
43. Hakansson, KEJ, Goossens, EAC, Trompet, S, van Ingen, E, de Vries, MR, van der Kwast, R, Ripa, RS, Kastrup, J, Hohensinner, PJ, Kaun, C, *et al.* (2018). Genetic associations and regulation of expression indicate an independent role for 14q32 snoRNAs in Human Cardiovascular Disease. *Cardiovascular research*.
44. Welten, SMJ, de Jong, RCM, Wezel, A, de Vries, MR, Boonstra, MC, Parma, L, Jukema, JW, van der Sluis, TC, Arens, R, Bot, I, *et al.* (2017). Inhibition of 14q32 microRNA miR-495 reduces lesion formation, intimal hyperplasia and plasma cholesterol levels in experimental restenosis. *Atherosclerosis* **261**: 26-36.
45. Boon, RA, Hofmann, P, Michalik, KM, Lozano-Vidal, N, Berghauer, D, Fischer, A, Knau, A, Jae, N, Schurmann, C, and Dimmeler, S (2016). Long Noncoding RNA Meg3 Controls Endothelial Cell Aging and Function: Implications for Regenerative Angiogenesis. *J Am Coll Cardiol* **68**: 2589-2591.
46. Bijkerk, R, Au, YW, Stam, W, Duijs, J, Koudijs, A, Liewers, E, Rabelink, TJ, and van Zonneveld, AJ (2019). Long Non-coding RNAs Rian and Miat Mediate Myofibroblast Formation in Kidney Fibrosis. *Front Pharmacol* **10**: 215.
47. Malnou, EC, Umlauf, D, Mouysset, M, and Cavaille, J (2018). Imprinted MicroRNA Gene Clusters in the Evolution, Development, and Functions of Mammalian Placenta. *Front Genet* **9**: 706.
48. Chiang, HR, Schoenfeld, LW, Ruby, JG, Auyeung, VC, Spies, N, Baek, D, Johnston, WK, Russ, C, Luo, S, Babiarz, JE, *et al.* (2010). Mammalian microRNAs: experimental evaluation of novel and previously annotated genes. *Genes & development* **24**: 992-1009.
49. Alon, S, Mor, E, Vigneault, F, Church, GM, Locatelli, F, Galeano, F, Gallo, A, Shomron, N, and Eisenberg, E (2012). Systematic identification of edited microRNAs in the human brain. *Genome Res* **22**: 1533-1540.
50. Ekdahl, Y, Farahani, HS, Behm, M, Lagergren, J, and Ohman, M (2012). A-to-I editing of microRNAs in the mammalian brain increases during development. *Genome Res* **22**: 1477-1487.

51. Gong, J, Wu, Y, Zhang, X, Liao, Y, Sibanda, VL, Liu, W, and Guo, AY (2014). Comprehensive analysis of human small RNA sequencing data provides insights into expression profiles and miRNA editing. *RNA Biol* **11**: 1375-1385.
52. Zheng, Y, Li, T, Ren, R, Shi, D, and Wang, S (2014). Revealing editing and SNPs of microRNAs in colon tissues by analyzing high-throughput sequencing profiles of small RNAs. *BMC Genomics* **15 Suppl 9**: S11.
53. Cho, S, Jang, I, Jun, Y, Yoon, S, Ko, M, Kwon, Y, Choi, I, Chang, H, Ryu, D, Lee, B, *et al.* (2013). MiRGator v3.0: a microRNA portal for deep sequencing, expression profiling and mRNA targeting. *Nucleic Acids Res* **41**: D252-257.
54. Eggington, JM, Greene, T, and Bass, BL (2011). Predicting sites of ADAR editing in double-stranded RNA. *Nat Commun* **2**: 319.
55. Betel, D, Koppal, A, Agius, P, Sander, C, and Leslie, C (2010). Comprehensive modeling of microRNA targets predicts functional non-conserved and non-canonical sites. *Genome Biol* **11**: R90.
56. Bhattacharya, A, and Cui, Y (2015). miR2GO: comparative functional analysis for microRNAs. *Bioinformatics (Oxford, England)* **31**: 2403-2405.
57. Mi, H, Muruganujan, A, Casagrande, JT, and Thomas, PD (2013). Large-scale gene function analysis with the PANTHER classification system. *Nat Protoc* **8**: 1551-1566.
58. Kim, D, Paggi, JM, Park, C, Bennett, C, and Salzberg, SL (2019). Graph-based genome alignment and genotyping with HISAT2 and HISAT-genotype. *Nature biotechnology* **37**: 907-915.
59. Pertea, M, Pertea, GM, Antonescu, CM, Chang, TC, Mendell, JT, and Salzberg, SL (2015). StringTie enables improved reconstruction of a transcriptome from RNA-seq reads. *Nature biotechnology* **33**: 290-295.
60. Liao, Y, Smyth, GK, and Shi, W (2019). The R package Rsubread is easier, faster, cheaper and better for alignment and quantification of RNA sequencing reads. *Nucleic Acids Res* **47**: e47.
61. Robinson, MD, McCarthy, DJ, and Smyth, GK (2010). edgeR: a Bioconductor package for differential expression analysis of digital gene expression data. *Bioinformatics (Oxford, England)* **26**: 139-140.
62. Ritchie, ME, Phipson, B, Wu, D, Hu, Y, Law, CW, Shi, W, and Smyth, GK (2015). limma powers differential expression analyses for RNA-sequencing and microarray studies. *Nucleic Acids Res* **43**: e47.
63. Wu, D, Lim, E, Vaillant, F, Asselin-Labat, ML, Visvader, JE, and Smyth, GK (2010). ROAST: rotation gene set tests for complex microarray experiments. *Bioinformatics (Oxford, England)* **26**: 2176-2182.
64. Baker, M, Robinson, SD, Lechertier, T, Barber, PR, Tavora, B, D'Amico, G, Jones, DT, Vojnovic, B, and Hodivala-Dilke, K (2011). Use of the mouse aortic ring assay to study angiogenesis. *Nat Protoc* **7**: 89-104.

CHAPTER 5

Supplemental Materials

Supplemental Figures

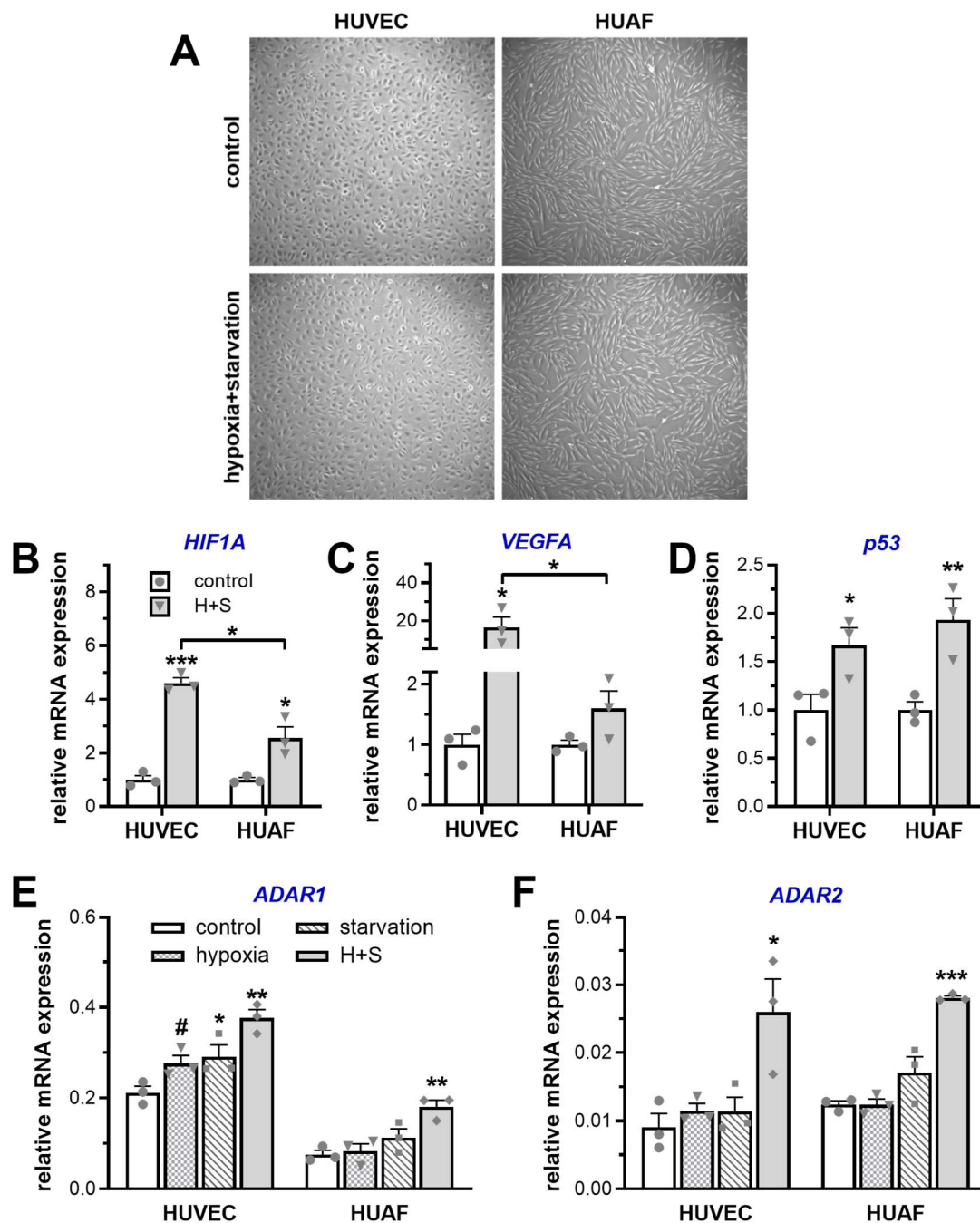
- I. In vitro ischemia conditions induce HIF1A, VEGFA, p53, ADAR1 and ADAR2 expression.
- II. MicroRNA expression and characterization of the microRNA qRT-PCR assays
- III. Expression of ADARs *in vitro* after knockdown and *in vivo* after hindlimb ischemia.
- IV. ADAR1 and ADAR2 expression in lower limb veins of patients with peripheral artery disease compared to coronary artery disease.
- V. Regulation of percentage miRNA editing after overexpression of either a WT-miRNA or an ED-miRNA.
- VI. Overall target gene regulation after overexpression of WT-miR-411-5p or ED-miR-411-5p.
- VII. Expression of validated WT-miRNA and ED-miRNA target gene in lower limb veins of patients with and without peripheral artery disease.
- VIII. Identification of vasoactive microRNAs containing tissue specific A-to-I editing

Supplemental Tables

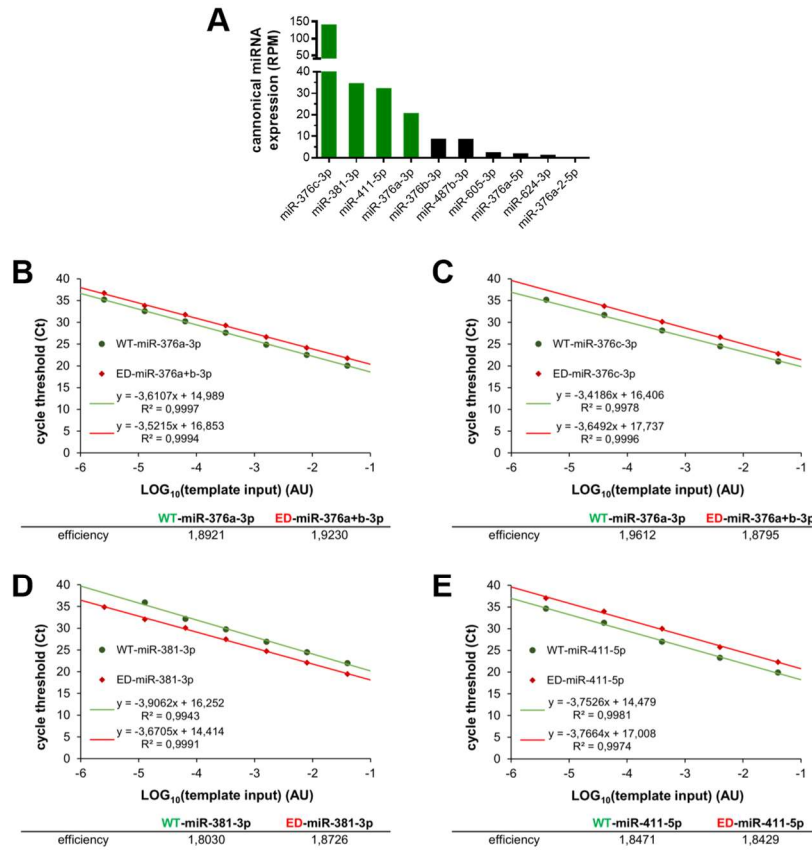
- I. MicroRNAs containing A-to-I editable adenosines
- II. Seed sequence analysis of A-to-I edited pri-miRNAs
- III. Overview of the findings per selected microRNA
- IV. Enriched pathways within putative targetomes
- V. Putative targets of WT-miRNAs or ED-miRNAs involved in one or more selected processes related to the response to ischemia
- VI. Number of miR-411-5p targets detected using RNA-seq and regulation of the unique targets
- VII. Number of targets within each targetome and fractions conserved in mice and detected by microarray
- VIII. Primer sequences and purpose
- IX. Sequences of WT-miRNA and ED-miRNA specific qRT-PCR assays
- X. Sequences of siRNA and synthesized endogenous 3'UTRs

Supplemental References

SUPPLEMENTAL FIGURES

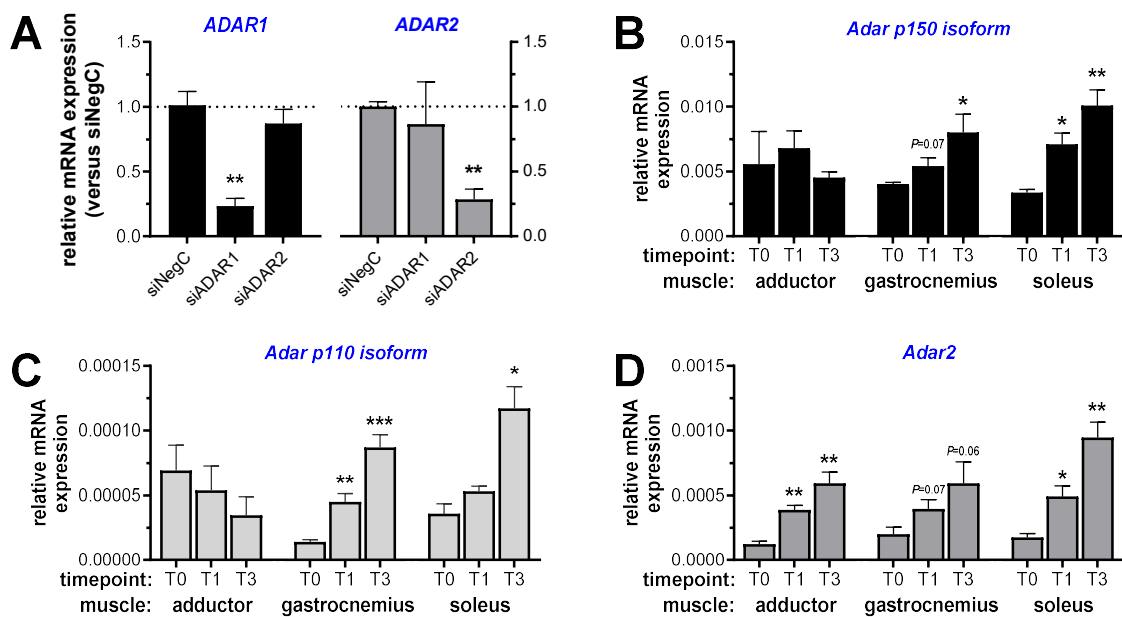


Supplemental Figure I: In vitro ischemia conditions induce HIF1A, VEGFA, p53, ADAR1 and ADAR2 expression. (A) Primary human umbilical vascular endothelial cells (HUVECs) and human umbilical arterial fibroblasts (HUAFs) were cultured either under normal or ischemic culture conditions, mimicked using a combination of hypoxia and serum starvation (H+S). Expression of hypoxia-inducible genes HIF1A (B) and VEGFA (C) and p53 (D) were successfully increased upon H+S culture conditions. (D-E) Regulation of ADAR1 (D) and ADAR2 (E) expression in response to either only serum starvation or hypoxia or the combination. All data are presented as mean \pm SEM (n=3). # P <0.1, * P <0.05, ** P <0.01, *** P <0.001; versus control condition unless otherwise indicated by 2-sided Student t test.

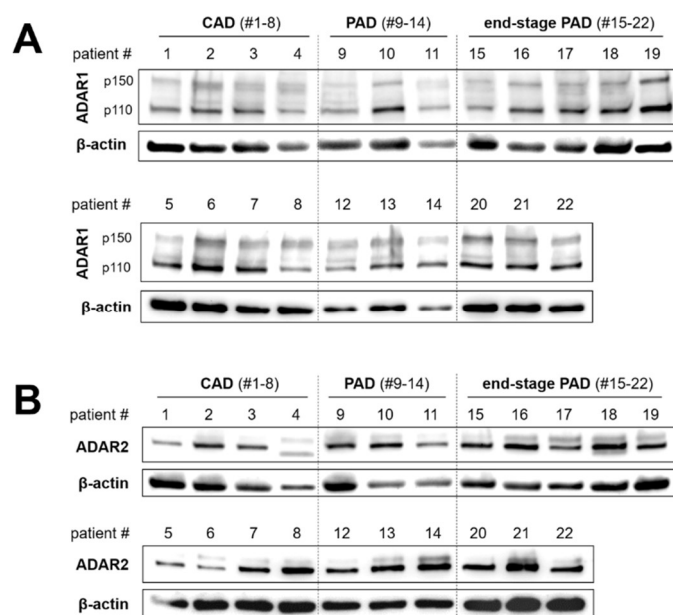


Supplemental Figure II: MicroRNA expression and characterization of the microRNA qRT-PCR assays. (A) Overall mature miRNA expression in reads per million (RPM) of microRNAs found edited at pri-miRNA level in vascular cells. Data are displayed in descending order and were extrapolated from miRbase.org (only canonical miRNA sequence reads were included). (B-E) Characterization of PCR efficiency of TaqMan WT-miRNA and custom ED-miRNA qRT-PCR kits by serial dilution of cDNA from HUAF samples transfected with 0.1 pg of the miRNA. To do so, cycle threshold was plotted versus the logarithmic function of the relative input. The equation: $\text{efficiency} = 10^{(-1/\text{slope})}$ was used to calculate the corresponding real-time PCR efficiencies¹.

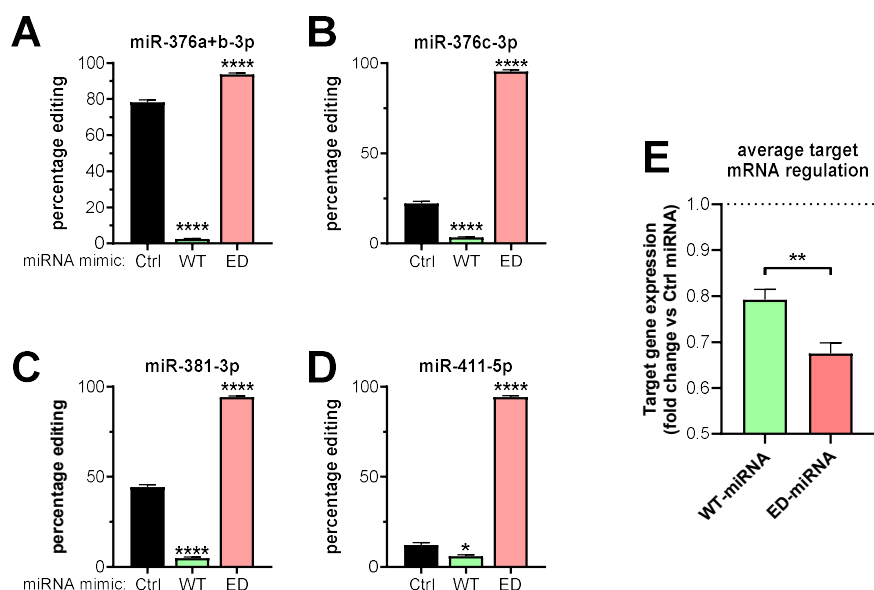
5



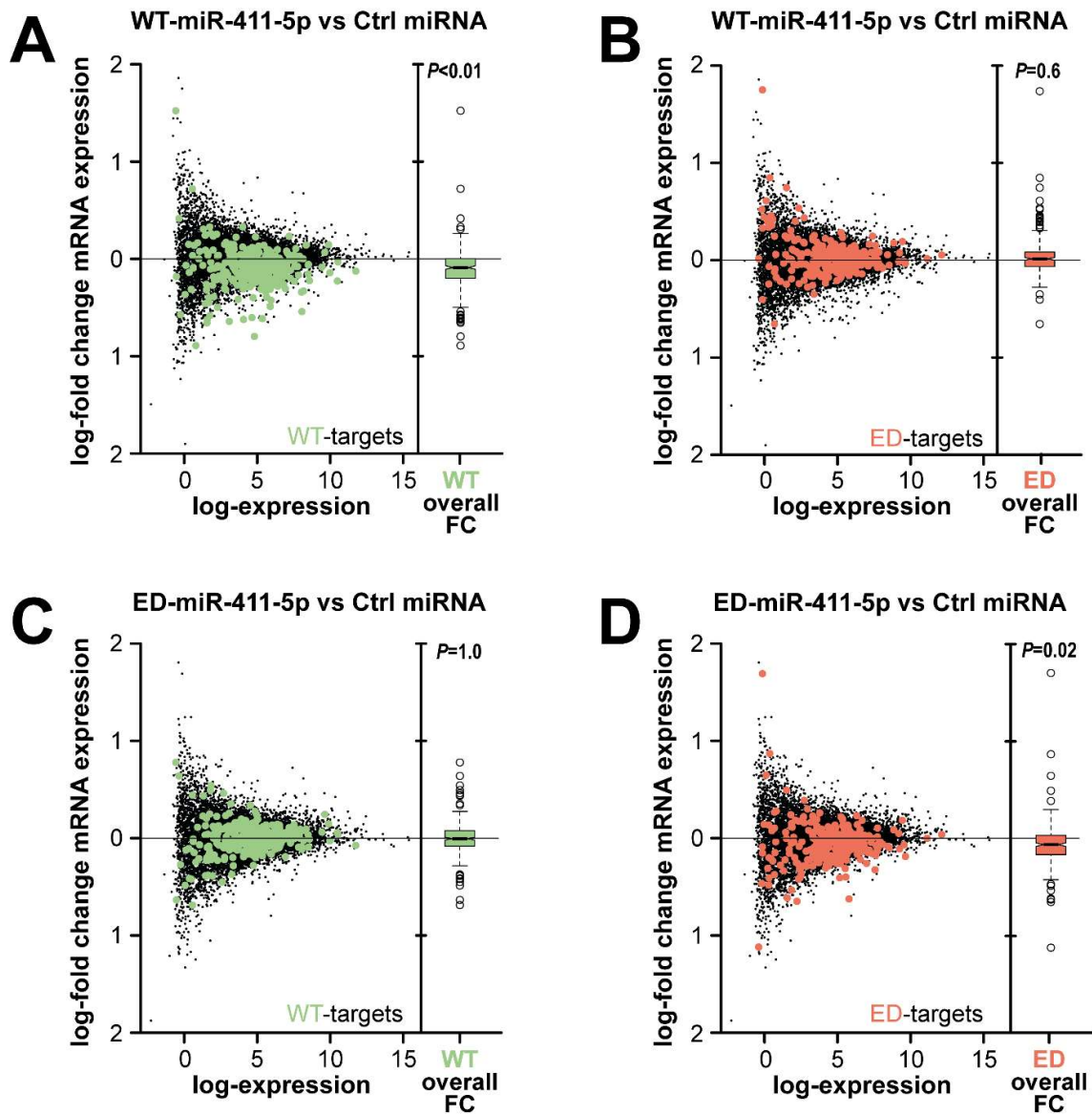
Supplemental Figure III: Expression of ADARs *in vitro* after knockdown and *in vivo* after hindlimb ischemia. (A) After transfecting HUAFs with a negative control, *ADAR1*-targeted or *ADAR2*-targeted siRNA (siNegC, siADAR1 and siADAR2 respectively), relative expression of *ADAR1* and *ADAR2* was measured by qRT-PCR to validate the knockdown efficiency and specificity. Data was expressed as fold change relative to siNegC and presented as mean \pm SEM (n=3 per treatment). (B-C) Relative expression of *Adar1* isoforms P150 (B) and P110 (C) and *Adar2* (D) in muscles before hindlimb ischemia (T0) and 1 and 3 days after (T1 and T3 respectively) as determined by qRT-PCR. Data was expressed relative to *Rplp0* and presented as mean \pm SEM (n=3 per treatment). * $P < 0.05$, ** $P < 0.01$, *** $P < 0.001$; versus siNegC or T0 by two-sided Student's *t*-test.



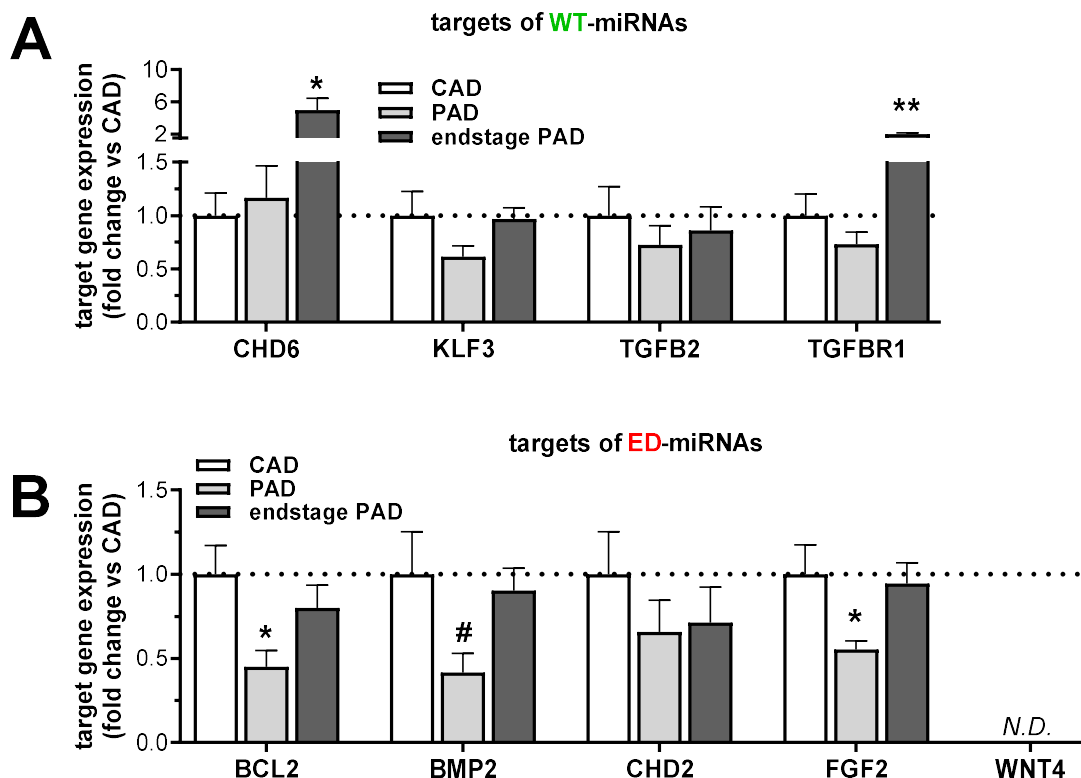
Supplemental Figure IV: ADAR1 and ADAR2 expression in lower limb veins of patients with peripheral artery disease compared to coronary artery disease. Westernblots of ADAR1 (A) and ADAR2 (B) expression in lower leg vein (LLV) samples from different patient groups. Normoxic LLV samples (n=8) from patients with coronary artery disease (CAD) undergoing coronary artery bypass-surgery were compared to ischemic LLV samples (n=6) from patients with peripheral artery disease (PAD) undergoing femoral artery to popliteal artery-bypass surgery and to critically ischemic LLV samples (n=8) from patients with end-stage PAD, undergoing lower limb amputation. Stable household gene beta-actin was used to normalize expression.



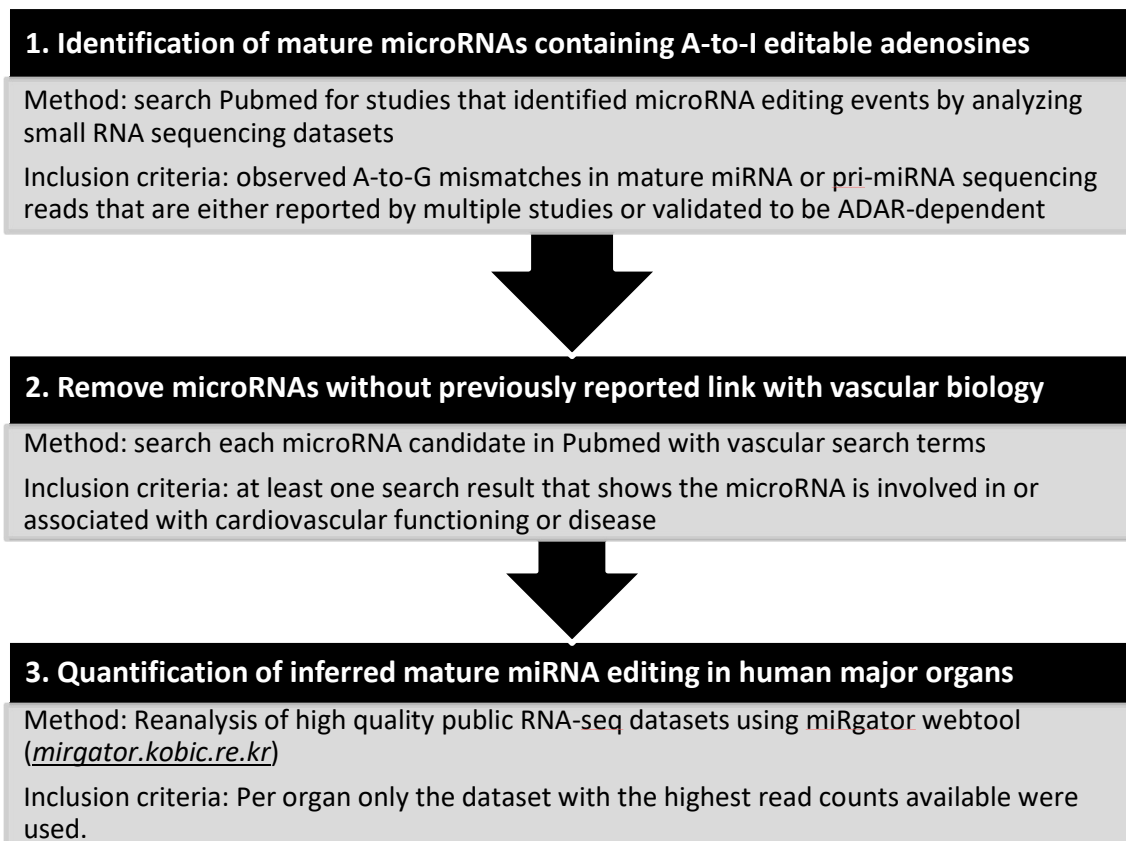
Supplemental Figure V: Regulation of percentage miRNA editing and average target mRNA regulation after overexpression of either a WT-miRNA or an ED-miRNA. HUAF samples were transfected with 0.1 μ g of either a WT-miRNA mimic (WT), an ED-miRNA mimic (ED) or a control miRNA mimic (Ctrl). (A-D) Percentage editing was calculated afterwards using version specific qRT-PCR assays. In each case, overexpression of WT-miRNA successfully reduced overall percentage editing compared to Ctrl and overexpression of ED-miRNA successfully increased percentage editing. Data are presented as mean \pm SEM (n=3). * P <0.05, **** P <0.0001 versus Ctrl mimic by 2-sided Student t test. (E) Average expression regulation of successful regulation of WT targets by WT-miRNA overexpression and ED targets by ED-miRNA overexpression shown in Figure 7C. Data are presented as mean \pm SEM. ** P <0.001 by 2-sided Student t test.



Supplemental Figure VI: Overall target gene regulation after overexpression of WT-miR-411-5p or ED-miR-411-5p. The log-fold changes (FC) of mRNA expression calculated from RNA-seq data obtained after overexpression of WT-miR-411-5p (A&B) or ED-miR-411-5p (C&D) compared to overexpression of a non-targeting control microRNA (Ctrl miRNA) in HUAFs. Data represent averages of 3 independent experiments and are visualized using mean-difference plots, highlighting the predicted target genes (with a 0.5 binding score threshold to minimize false positives, see **Supplemental Table VI**) that were uniquely targeted by the WT-miR-411-5p (green, A&C) or ED-miR-411-5p (red, B&D). The overall distribution of the logFC per targetome is shown in the boxplots. Differential expression of each targetome was tested using ROAST².



Supplemental Figure VII: Expression of validated WT-miRNA and ED-miRNA target gene in lower limb veins of patients with and without peripheral artery disease. (A&B) Relative mRNA expression of genes we validated (see Figure 7B&C) to be targeted by the four selected WT-miRNAs (A) or ED-miRNAs (B) in lower leg vein (LLV) samples from different patient groups. LLV samples from patients with coronary artery disease (CAD) but not peripheral artery disease (PAD) (n=8) were compared to LLV samples from patients with severe PAD (n=6) and LLV samples from patients with end-stage PAD (n=8). Expression was normalized to stable household gene RPLP0 and expressed as fold change of the CAD group. Expression of WNT4 was not detected (N.D.) in these samples. Data is presented as mean \pm SEM. *P<0.05, **P<0.01; by 2-sided Student t test versus CAD.



Supplemental Figure VIII: Identification of vasoactive microRNAs containing tissue specific A-to-I editing. A schematic overview of the steps taken to identify vasoactive microRNAs that can be A-to-I edited in a tissue and context dependent manner, using manual literature curation and reanalysis of public RNA-seq datasets.

SUPPLEMENTAL TABLES

Supplemental Table I. MicroRNAs containing A-to-I editable adenosines

#	A-to-I editable miRNAs	Chromosome	Dominant side of miRNA duplex	Sequence and editable adenosines	Pubmed ID linking miRNA to vascular functioning	Source of reported A-to-I editing in non-vascular tissue
1	miR-376a1-3p	14	3p	AUCAU A AGGAAAAUCCACGU	28968594	Kawahara et al. Science 2007; Kawahara et al. 2008
2	miR-376a2-3p	14	3p	AUCAU A AGGAAAAUCCACGU	28968594	Kawahara et al. Science 2007; Pinto et al. 2017
3	miR-376b-3p	14	3p	AUCAU A AGGAAAAUCCAUUU	22248718	Kawahara et al. Science 2007; Kawahara et al. 2008
4	miR-376c-3p	14	3p	AACA A AGGAAAAUCCACGU	24216752	Alon et al. 2012; Wang et al. 2017
5	miR-381-3p	14	3p	UA A ACAAGGGCAAGCCUCUCUGU	29540663	Alon et al. 2012; Wang et al. 2017
6	miR-411-5p	14	5p	UAG A AGACCCGUUAUGCCUACG	25832031	Kawahara et al. 2008; Chiang et al. 2010; Wang et al. 2017
7	miR-376a2-5p	14	3p	GU A GAUUUCCUUCUAUGGU	26912672	Kawahara et al. Science 2007; Wang et al. 2017
8	miR-605-3p	10	3p	AGA A GGCAUAUGAGAUUUAGA	29221163	Pinto et al. 2017; Li et al. 2018
9	miR-624-3p	14	5p	CACA A GGUAUUUGUAUUACCU	26149483	Pinto et al. 2017; Li et al. 2018
10	miR-487b-3p	14	3p	A A UCGUACAGGGCAUCCACUU	25085941	Van der Kwast et al. 2018
11	Let-7c-5p	21	5p	UG A GGUAGUAGGUUUGUAUGGUU	25814653	Pinto et al. 2017; Li et al. 2018
12	Let-7d-3p	9	5p	CU A U A CGACCCGUCGCCUUUCU	25814653	Pinto et al. 2017; Li et al. 2018
13	Let-7e-3p	19	5p	CU A U A CGGCCUCCUAGCUUUCC	28195197	Alon et al. 2012; Pinto et al. 2017
14	miR-24-2-5p	19	3p	UG C CU A CU G AGCUGAAACACAG	24583309	Alon et al. 2012; Ekdahl et al. 2012
15	miR-27a-5p	19	3p	A GGCCU A GCUGCUUGUGAGCA	26892968	Pinto et al. 2017; Li et al. 2018
16	miR-27a-3p	19	3p	UU C ACA G UGGCCUAAGUCCGC	25814653	Pinto et al. 2017; Li et al. 2018
17	miR-98-5p	X	5p	UG A GGU A UA A GUUGUAUUGUU	26367177	Pinto et al. 2017; Ishiguro et al. 2018
18	miR-99a-5p	21	5p	A ACCC G UA G AUCCGAUCUUGUG	27403035	Wang et al. 2017; Pinto et al. 2017
19	miR-130b-3p	22	3p	C A GUG C AAUGAUGAAAGGG C AU	24898744	Pinto et al. 2017; Li et al. 2018
20	miR-151a-3p	8	5p	CU A G A CGU A AGCCUCCUUGAGG	26149483	Kawahara et al. EMBO Rep. 2007; Wang et al. 2017
21	miR-200b-3p	1	3p	UA A U A CGCCUUGGUAAUGAUGA	25814653	Alon et al. 2012; Wang et al. 2017
22	miR-337-3p	14	3p	CU C CU A U A UGAUGCCUUUCUUC	28461247	Wang et al. 2017; Pinto et al. 2017
23	miR-376a1-5p	14	3p	GU A GAUUUCCUUCUAUGAGUA	26912672	Kawahara et al. Science 2007; Choudhury et al. 2012
24	miR-377-3p	14	3p	AUC C ACA A AGGCAACUUUUGU	26912672	Pinto et al. 2017; Li et al. 2018
25	miR-378a-3p	5	3p	ACUG G ACUUGGAGUC A GAAGGC	25814653	Alon et al. 2012; Pinto et al. 2017
26	miR-379-5p	14	5p	UG G U A GCUAUGGAACGUAGG	26912672	Wang et al. 2017; Pinto et al. 2017
27	miR-421-3p	X	3p	AUCA A CA G ACAUA A AUUGGGCGC	22952991	Alon et al. 2012; Tomaselli et al. 2015
28	miR-455-5p	9	3p	UAUG G CCUUUGGACU A UCG	25686251	Alon et al. 2012; Warnefors et al. 2014; Tomaselli et al. 2015
29	miR-494-3p	14	3p	UG A AAC A UACACGGGA A ACCUC	25085941	Voellenke et al. 2012; Li et al. 2018
30	miR-497-5p	17	5p	C A GC A GCACACUGUGGUUUU G	28122380	Alon et al. 2012; Warnefors et al. 2014; Tomaselli et al. 2015; Wang et al. 2017; Pinto et al. 2017
31	miR-497-3p	17	5p	C A AAC C ACACUGUGGUUU A	25814653	2015; Wang et al. 2017; Pinto et al. 2017
32	miR-503-5p	X	5p	U A GC A CGGGAAACAGUUCUGCAG	24583309	Tomaselli et al. 2015; Pinto et al. 2017
33	miR-539-5p	14	3p	AG A AAU A UCCUUGGGUG	27981363	Alon et al. 2012; Pinto et al. 2017
34	miR-589-3p	7	5p	UC A GA A CA A AUGCCGGUUCCAGA	23465244	Alon et al. 2012; Wang et al. 2017
35	miR-1260b-5p	11	5p	AU C CC A CC A CGCCACCAU	23746831	Pinto et al. 2017; Kebria et al. 2016
36	miR-1251-5p	12	5p	ACU C U A GCUGGCCAAAGCGCGCU	-	Wang et al. 2017; Pinto et al. 2017
37	miR-1295b-3p	1	5p	AAU A GG C CA G GAUCUGGGCAA	-	Wang et al. 2017; Paul et al. 2017
38	miR-1301-3p	2	3p	UUG C AG C UGCCUGGGAGUGACUUC	-	Wang et al. 2017; Pinto et al. 2017
39	miR-1304-3p	11	5p	UCU C AC G UAGCCUCCGAACCC	-	Wang et al. 2017; Pinto et al. 2017
40	miR-301a-3p	17	3p	C A GUG C AAUAGUAUUGUCA A AGC	-	Pinto et al. 2017; Li et al. 2018
41	miR-301b-3p	22	3p	C A GUG C AAUGAUAUUGUCA A AGC	-	Pinto et al. 2017; Li et al. 2018
42	miR-3144-3p	6	5p	AU A U A CCU G UUCGGUCUCUUUA	-	Wang et al. 2017; Li et al. 2018
43	miR-3157-3p	10	5p	CUG C CU A AGUCU A GCUGAAGCU	-	Tomaselli et al. 2015; Pinto et al. 2017
44	miR-3167-3p	11	5p	AG G AUU C AGAAAUACUGGUGU	-	Pinto et al. 2017; Ishiguro et al. 2018
45	miR-3622a-3p	8	5p	UCA C CU G ACCCUCCAUCCUGU	-	Wang et al. 2017; Pinto et al. 2017; Li et al. 2018
46	miR-3681-5p	2	unclear	U A GU G GAU G AGUACACUCUGUC	-	Pinto et al. 2017; Paul et al. 2017
47	miR-378b-3p	3	3p	ACUG G ACUUGGAGGCAGAA A	-	Pinto et al. 2017; Li et al. 2018
48	miR-378c-5p	10	5p	ACUG G ACUUGGAGUACGA A AGUGG	-	Pinto et al. 2017; Li et al. 2018
49	miR-4510-5p	15	5p	UG A GGG A UAGG A UGUAUGGUU	-	Pinto et al. 2017; Li et al. 2018
50	miR-4662a-5p	8	5p	UU A GCC A AUUGUCCAUCUUUAG	-	Pinto et al. 2017; Li et al. 2018
51	miR-488-3p	1	3p	UUG A AG G CUAUUUUCCUGGUC	-	Pinto et al. 2017; Li et al. 2018
52	miR-532-5p	X	3p	CAUG C CU G AGUGU A GGACCGU	-	Wang et al. 2017; Pinto et al. 2017
53	miR-556-3p	1	5p	AUAU A CCA A UAGCCUACUUCUU	-	Pinto et al. 2017; Li et al. 2018
54	miR-561-3p	2	5p	CA A AG U UU A GAUCCUUGAAGU	-	Pinto et al. 2017; Li et al. 2018
55	miR-598-3p	8	3p	U A CGU C AUCGUUGUCAUCGUCA	-	Alon et al. 2012; Pinto et al. 2017
56	miR-625-3p	14	5p	G A CU A U A GAACUUUCCCCUCA	-	Pinto et al. 2017; Li et al. 2018
57	miR-6503-3p	11	unclear	GGG A CU A GGAGUAGCAGACUCC	-	Wang et al. 2017; Pinto et al. 2017
58	miR-664a-5p	1	3p	ACUG G CU A GGGAAAUGAUUGGAU	-	Wang et al. 2017; Pinto et al. 2017
59	miR-944-3p	21	3p	AAU A U A UUGUAUCAUCGGAUGAG	-	Pinto et al. 2017; Li et al. 2018
60	miR-99b-3p	19	5p	CA A GC C UGUGUCUGGGUCCG	-	Pinto et al. 2017; Paul et al. 2017

Supplemental Table II. Seed sequence analysis of A-to-I edited pri-miRNAs

miRNA	WT-miRNA sequence and pri-miRNA A-to-I editing location	WT-miRNA seed	Seed sequence shared by	ED-miRNA seed	Seed sequence shared by
miR-376a1-5p	GU A GAUUCUCCUUCUAUGAGUA	UAGAUUC	none	UGGAUUC	none
miR-376a1-3p	AUCAU A GAGGAAAAUCCACGU	UCAUAGA	miR-376a2+b-3p	UCAU G GA	none
miR-376a2-5p	GGU A GAUUUCCUUCUAUGGU	GUAGAUU	none	GUGGAUU	miR-8056*
miR-376a2-3p	AUCAU A GAGGAAAAUCCACGU	UCAUAGA	miR-376a1+b-3p	UCAU G GA	none
miR-376b-3p	AUCAU A GAGGAAAAUCCAUGUU	UCAUAGA	miR-376a1+a2-3p	UCAU G GA	none
miR-376c-3p	AACA A GAGGAAAAUCCACGU	ACAUAGA	none	ACAU G GA	miR-4802-3P*
miR-381-3p	UAU A CAAGGGCAAGCUCUCUGU	AUACAAG	miR-300-3p	AUG C AAG	none
miR-411-5p	UAGU A GACCGUAUAGCGUACG	AGUAGAC	none	AGU G GAC	none
miR-605-3p	AGA A GGCACUAUGAGAUUUAGA	GAAGGCA	none	GAG G GCA	miR-3616-3p*
miR-624-3p	CACA A GGUAUUGGUAUUACCU	ACAAGGU	none	ACA G GGU	none
miR-487b-3p [†]	AA A UCGUACAGGGUCAUCCACUU	AUCGUAC	none	G UCGUAC	none

* unvalidated microRNA according to Targetscan².

[†] characterized previously by Van der Kwast et al. 2018³.

Supplemental Table III. Overview of the findings per selected microRNA

Experiment	Figure	Tissue	miR-376a&b-3p			miR-376c-3p			miR-381-3p			miR-411-5p		
			WT	ED	% editing	WT	ED	% editing	WT	ED	% editing	WT	ED	% editing
primary miRNA editing	2	HUVECs HUAFs	≈	++	+	+	++	++	+	+	+	++	+	
mature miRNA editing	3	HUVECs HUAFs HUAFs	≈	+	≈	+	++	+	≈	+	+	+	+	
AGO2 IP		HUAFs	+	++	+	++	++	+	++	++	+	+	≈	
hindlimb ischemia (adductor remains relatively normoxic)	5	adductor gastrocnemius soleus	excluded because edited adenosine is not conserved in the murine mmu-miR-376a-3p			+	≈/-	-	≈/+	-	≈	++	≈	
ex vivo culture	6	IMA VSM	+	++	+	+	+	≈/+	+	+	+	+	≈/+	
ischemic LLVs (PAD patients) versus normoxic LLVs (CAD patients)	6	PAD patient LLVs end-stage PAD patient LLVs	++	++	≈/+	+	+	+	+	+	++	++	≈/+	
role of ADARs	primary miRNA editing	HUAFs siADAR1 HUAFs siADAR2 HUAFs siADAR1 HUAFs siADAR2	≈	-	≈	-	--	-	≈/-	--	-	-	--	
			+	-	-	-	-	≈	-	-	-	-	≈/-	
			-	≈/-	+	-	--	-	-	-	-	-	-	≈
			≈/-	-	-	-	-	≈	-	≈/-	≈	-	≈	≈
<i>in vitro</i> angiogenesis	wound healing	HUAFs	-	+	++	-	-	≈	≈/-	+	+	+	+	
	tube formation	HUVECs	≈/-	≈/-	≈	-	≈/+	++	≈/-	+	+	+	≈/-	
neovessel sprouting	8	aortic segments	not conserved in mmu-miR-376a			≈/-	+	++	≈/+	+	+	+	++	

Supplemental Table IV. Enriched pathways within putative targetomes*

	Total genes mapped to pathway	# of mapped genes in target set	Expected # of genes targeted	Fold Enrichment	<i>P</i> value
WT-miR-376a+b-3p					
-					
ED-miR-376a+b-3p					
Cadherin signalling pathway	158	24	8.06	2.98	0.0007
Wnt signalling pathway	312	34	15.91	2.14	0.0062
WT-miR-376c-3p					
-					
ED-miR-376c-3p					
Cadherin signalling pathway	158	27	11.87	2.27	0.0395
WT-miR-381-3p					
-					
ED-miR-381-3p					
Cadherin signalling pathway	158	25	9.83	2.54	0.0046
Wnt signalling pathway	312	43	19.41	2.22	0.0010
WT-miR-411-5p					
Cadherin signalling pathway	158	23	4.94	4.66	0.0000
Wnt signalling pathway	312	31	9.76	3.18	0.0000
ED-miR-411-5p					
-					

* Putative targetomes were analyzed by the PANTHER pathway algorithm⁴. Only pathway enrichments with $P < 0.05$ after Bonferroni correction are reported.

Supplemental Table V. Putative targets of WT-miRNAs or ED-miRNAs involved in one or more selected processes related to the response to ischemia

Spreadsheets are too large for print, but can be requested.

Supplemental Table VI: Number of miR-411-5p targets detected using RNA-seq and regulation of the unique targets

Targetome	>0.5 binding score	Detected in RNA-seq	Unique to either targetome	Fraction down regulated	Fraction up regulated	Direction	P-Value	FDR
WT-miR-411-5p overexpression vs Ctrl microRNA overexpression								
WT	464	348	300	0.3133	0.0300	Down	0.002	0.003
ED	407	315	274	0.0547	0.0876	Up	0.579	0.579
ED-miR-411-5p overexpression vs Ctrl microRNA overexpression								
WT	464	348	300	0.0733	0.0767	Down	0.987	0.987
ED	407	315	274	0.2299	0.0657	Down	0.022	0.043
ED-miR-411-5p overexpression vs WT-miR-411-5p overexpression								
WT	464	348	300	0.0300	0.3333	Up	0.001	0.001
ED	407	315	274	0.2482	0.0438	Down	0.013	0.013

Overall regulation of unique targets was examined using limma's roast function³⁸

Supplemental Table VII: Number of targets within each targetome and fractions conserved and detected

microRNA	target set	human	no cutoff				0.5 score cutoff			
			conserved in mouse		detected in array		conserved in mouse		detected in array	
miR-376c	WT only	879	590	67%	406	69%	218	37%	157	39%
	ED only	1200	854	71%	609	71%	266	31%	190	31%
	shared	326	207	63%	146	71%	45	22%	36	25%
miR-381	WT only	1259	959	76%	698	73%	509	53%	376	54%
	ED only	886	557	63%	391	70%	169	30%	125	32%
	shared	387	248	64%	185	75%	68	27%	51	28%
miR-411	WT only	557	256	46%	176	69%	58	23%	43	24%
	ED only	590	307	52%	218	71%	67	22%	49	22%
	shared	85	37	44%	28	76%	1	3%	1	4%

Supplemental Table VIII: Primer sequences and purpose

Primer	Used for:	Sequence (5' to 3')
pri-miR-let7c_F	amplification & sequencing	TTGGAGGAGCTGACTGAAGAT
pri-miR-let7c_R		ATGAAGAATTCCCTCGACGGCT
pri-miR-let7d_F	amplification & sequencing	TTTGAAGTGCATCTGCCAAGT
pri-miR-let7d_R		GCAAGGAAACAGGTTATCGGT
pri-miR-let7e_F	amplification & sequencing	TGGTCCCTGTCTGTCTGTCT
pri-miR-let7e_R		TAAGGGTCCCTGAGTGGGG
pri-miR-1260b_F	amplification & sequencing	CAGGTGCTTACCGCAATCAG
pri-miR-1260b_R		CTCCAAGCAGCAGCAACAG
pri-miR-130b_F	amplification & sequencing	AGCCTGCATTCCAGGTCTCAG
pri-miR-130b_R		AGGCAGCAAGCTCCCTTTCC
pri-miR-151a_F	amplification & sequencing	CTACAGTAGCTGAGCCTGGT
pri-miR-151a_R		AGGTTTGGGCAACACCGA
pri-miR-200b_F	amplification & sequencing	CAGCTACTGAGCTTCCCAGC
pri-miR-200b_R		TCGGCCGGTCGCTGC
pri-miR-24-2_F	amplification & sequencing	CCGCTGTCCCCTGC
pri-miR-24-2_R		CAGCCACCCAGGGAAG
pri-miR-27a_F	amplification & sequencing	CTGAGCTCTGCCACCGAG
pri-miR-27a_R		GCAAGGCCAGAGGAGGTGAG
pri-miR-337_F	amplification & sequencing	ATCCGAGCGCTTGCACTG
pri-miR-337_R		AAGGGTGCAGAGGAGGGTC
pri-miR-376a1_F	amplification; qPCR & sequencing	TTTCTGATGACTCAAGCACAGG
pri-miR-376a1_R		CGTCCCTCCGAGGTTTCAAAG
pri-miR-376a2_F	amplification & sequencing	TTGTGTTTGGATGTACTTAGG
pri-miR-376a2_R		CCTGATGGTGGCTTCAGTCC
pri-miR-376b_F	amplification & sequencing	ACTGTGTTTCCAGATTTGTCTTTCC
pri-miR-376b_R		TCAGGCCCTACGGTCTCTTC
pri-miR-376c_F	amplification & sequencing	ATTTTGATAGATTGTGCTTAGGTTC
pri-miR-376c_R		AGGAATGTTTCCAAGCAGCA
pri-miR-377_F	amplification & sequencing	GGCATCTCGGTGTGTCTTTG
pri-miR-377_R		GGGGTGTAGATGCCCTGAG
pri-miR-378a_F	amplification & sequencing	GGAGTGAGCGGCTTGTATGG
pri-miR-378a_R		GTGGGGAAGGTGACTCCACT
pri-miR-379_F	amplification & sequencing	GTGACGCCAACTTCAGGGG
pri-miR-379_R		GTTGGCAACACCTCCAGGAA
pri-miR-381_F	amplification & sequencing	CCGTGAATGATAGTGAGAAC
pri-miR-381_R		ACACATACCGCATCCCTTG
pri-miR-411_F	amplification; qPCR & sequencing	AAGGCCTTGGAGGGCTTTCTG
pri-miR-411_R		GACAGCGTTGTTCCAGGAGC
pri-miR-487b_F	amplification; qPCR & sequencing	GAAGACGTACCAAGTCCACCC
pri-miR-487b_R		GCTCCAGAGTCTGCGCTCTT
pri-miR-494_F	amplification & sequencing	TTCGGCAGTTCTGTTTTGAT
pri-miR-494_R		TCCAGGGTGGGATTTGATACT
pri-miR-497_F	amplification & sequencing	TGGGGTCTTCCCAGCACT
pri-miR-497_R		TCCCAGGGCCAAGCCTC
pri-miR-503_F	amplification & sequencing	TATTCCTGGCTAGGCTGGGG
pri-miR-503_R		ACTTACCTGCTGGGTAGGC
pri-miR-539_F	amplification & sequencing	TCACCATCTAACCTTGAGCCAAA
pri-miR-539_R		ATGGCGTCCAGGAAGTCTGC
pri-miR-589_F	amplification & sequencing	AGCCTGAGAGCCGACCCT
pri-miR-589_R		GCAGAAGGCAGGAATCCAGAG
pri-miR-605_F	amplification & sequencing	GAAC TTTGGTAGAACTTTACAGC
pri-miR-605_R		CTGTAACATAGGTACCTGTATCTG

pri-miR-624_F	amplification & sequencing	GGTTTGTGTTCTTGTAATGAAAAA
pri-miR-624_R		ATCTTGTTCAC TGAAACCACTT
pri-miR-98_F	amplification & sequencing	AAAGAGTCTGTCACCATGTAAAA
pri-miR-98_R		TGCTAAGACTAAGTGTGAATATGCC
pri-miR-99a_F	amplification & sequencing	TTTTGACTCTTAATTGCATCAGATA
pri-miR-99a_R		GCACTGTGTATAGCATTTTTGTCA
pri-miR-376a2_F	qPCR	CGTGCTTTCGGGATGAAAC
pri-miR-376a2_R		CAGTCCAGCCATGATCCCAA
pri-miR-376b_F	qPCR	CAGAGCCCAGTCCCTTCTTTG
pri-miR-376b_R		CCTACGGTCTCTTCCAGAAACA
pri-miR-376c_F	qPCR	GGTTCATGCTTTCAGGACTCA
pri-miR-376c_R		TCTTCCCTGATGGTGGTTTCAG
pri-miR-381_F	qPCR	AACCTGCCCAGTGCTATTGTT
pri-miR-381_R		ACACACATAACCGCATCCCTT
pri-miR-605_F	qPCR	TGTCTCTAGCCCTAGCTTG GTT
pri-miR-605_R		AGCAATATAACCTGTGGCTGTCA
pri-miR-624_F	qPCR	AAAGTGGTTTTGTGTTCTTGTAATG
pri-miR-624_R		ACCACTTAGGTGTAATGCTATCTCA
U6-F	qPCR	AGAAGATTAGCATGGCCCT
U6-R		ATTTTGCGTGCATCCTTGCG
ADAR1_human_F	qPCR	GCTTGGGAACAGGGAATCGC
ADAR1_human_R		CGCAGTCTGGGAGTTGTATTTT
ADAR2_human_F	qPCR	GGAAGCTGCCTTGGGATCAG
ADAR2_human_R		GCTGCTGGAAC TCATGTTTTCTTC
RPLP0_human_F	qPCR	TCTCTGTTGAAAGTGACATCG
RPLP0_human_R		TGTCTGCTCCACAATGAAAC
p53_F	qPCR	TGACACGCTTCCCTGGATTG
p53_R		TTTTCAGGAAGTAGTTTTCCATAGGT
VEGFa_F	qPCR	ATCACCATGCAGATTATGCGG
VEGFa_R		CCCCTTCCCTTTCCTCGAAC
HIF1A_F	qPCR	TGTCTCTAGCCCTAGCTTG GTT
HIF1A_R		AGCAATATAACCTGTGGCTGTCA
Adar1p150_mouseF	qPCR	GGCACTATGTCTCAAGGGTTC
Adar1p150_mouseR		CCTGTGGCTGCGGGTATC
Adar1p110_mouseF	qPCR	TCACCAATCTGCGCCCTAAC
Adar1p110_mouseR		GTGTCTGGTGAGGGAACACC
Adar2_mouse_F	qPCR	GCTTGCCCTGAAGGAGTTTTG
Adar2_mouse_R		CAGTGCTGCTGGAAC TCATATTC
Rplp0_mouse_F	qPCR	GCGACCTGGAAGTCCAACTA
Rplp0_mouse_R		ATCTGCTGCATCTGCTTGG
ANGPT2_3'UTR_F	construct cloning (WT-376a&b site)	CTCTCTCGAGTATCAACAGAAACGTGCCAT
ANGPT2_3'UTR_R		CTGCGGCCGCGGGTGAATCTTGAGACATATAGC
WNT4_3'UTR_F	construct cloning (ED-376a&b site)	CTCTCTCGAGCTGAAGTCCCACCCTAGAACC
WNT4_3'UTR_R		CTGCGGCCGCGTTTGTCTGCTTCCCAGGACT
TGFBR2_3'UTR_F	construct cloning (WT-376c site)	CTCTCTCGAGACTGTTCTATAGTTTTTTCAGGATCT
TGFBR2_3'UTR_R		CTGCGGCCGCATTCAAACATGACCATGCTAATAA
CHD2_3'UTR_F	construct cloning (ED-376c site)	CTCTCTCGAGGGGGGATGAGACCATGAGATT
CHD2_3'UTR_R		CTGCGGCCGCTGTGCTAAGAACTTTTCTCCCT
KLF3_3'UTR_F	construct cloning (WT-381 site)	CTCTCTCGAGATGAAGTTGCTCCGAGCTGTC
KLF3_3'UTR_R		CTGCGGCCGCTCCCATTTGGACTACAGAGTAGAAAC
CHD6_3'UTR_F	construct cloning (WT-411 site)	CTCTCTCGAGTCTAAAAAGTCATGATTC CCCCACT
CHD6_3'UTR_R		CTGCGGCCGCGGCTCTGTTGGGCTAACG
TGFB2_3'UTR_F	construct cloning (WT-411 site)	CTCTCTCGAGTTTGCCACATCATTCAGAGAAG
TGFB2_3'UTR_R		CTGCGGCCGCCCTATCTGAGAGGAAAATGTCTGC
FGF2_3'UTR_F	construct cloning	CTCTCTCGAGTATTGCATCTGCTGTTACCCAG

FGF2_3'UTR_R	(ED-411 site)	CTGCGGCCGC	CGTCCTGAGTATTCGGCAAC
ANGPT2_F	qPCR	CAGCCCCACGTGTCCAATG	
ANGPT2_R		GCCGTCTGGTTCTGTACTGC	
BMP2_F	qPCR	CCAGACCACCGGTTGGAG	
BMP2_R		AAACTCCTCCGTGGGGATAG	
WNT4_F	qPCR	GCTCCACACTCGACTCCTTG	
WNT4_R		CCCATGCACTGTCTGTAC	
TGFBR1_F	qPCR	TCCTCGAGATAGGCCGTTG	
TGFBR1_R		CCAGTTCCACAGGACCAAGG	
CHD2_F	qPCR	ATGCAAGACTGGATTTCTGAAG	
CHD2_R		TCTCACGGCATAACCATGC	
BCL2_F	qPCR	AACATCGCCCTGTGGATGAC	
BCL2_R		GGGCCAAACTGAGCAGAGTC	
KLF3_F	qPCR	TGACCCAGTTCTGTCAAGC	
KLF3_R		TGTATTCCGTGCGACAGACC	
CHD6_F	qPCR	GCTCTGGTTGCCATCCTTCTG	
CHD6_R		CCACCTTCGTCTGTGTAAGT	
TGFB2_F	qPCR	CCCTGCTGCACTTTTGTACC	
TGFB2_R		AGGAGATGTGGGGTCTTCCC	
FGF2_F	qPCR	ACCTGGCTATGAAGGAAGATGG	
FGF2_R		CGTTTCAGTGCCACATACCAAC	

Gray highlighted sequences are primer extensions to flank the amplicon restriction enzyme sites

Supplemental Table IX. Sequences of custom ED-miRNA specific qRT-PCR assays

Assay target	Component	Sequence
ED-miR-376a+b-3p	hairpin RT primer	GTGCTAACGTGTGCAGGGACGGAGGACACGTTAGCACACGTTGG
	qPCR primers	CCGGCGATCATGGAGGAAAATC TGCAGGGACGGAGGA
	qPCR probe	<VIC>ACGTTAGCACACGTTGGAT<MGB>
ED-miR-376c-3p	hairpin RT primer	GTCGTATCCAGTGCAGGGACCGAGGACTGGATACGACACGTTGG
	qPCR primers	CCGGCGAACATGGAGGAAATTC TGCAGGGACCGAGGA
	qPCR probe	<VIC>CTGGATACGACACGTTGGAA<MGB>
ED-miR-381-3p	hairpin RT primer	GGCGTTGGCAGTGCAGGGTCCGAGGTCTGCCAACGCCACAGAG
	qPCR primers	GCCGTATGCAAGGGCAAGC GTGCAGGGTCCGAGG
	qPCR probe	<VIC>CCAACGCCACAGAGAG<MGB>
ED-miR-411-5p	hairpin RT primer	GTCGTATCCAGTGCAGGGACCGAGGACTGGATACGACCGTACGC
	qPCR primers	CCGCCTAGTGGACCGTATAGC TGCAGGGACCGAGGA
	qPCR probe	<VIC>CTGGATACGACCGTACGCT<MGB>

<VIC>, VIC fluorophore; <MGB>, minor groove binder

Supplemental Table X: Sequences of siRNA and synthesized endogenous 3'UTRs

siRNA	targets	sequence
siADAR1	ADAR1	5'-GCUAUUUGCUGUCGUGUCA (dT) (dT) -3'
siADAR2	ADAR2	5'-GAUCGUGGCCUUGCAUUA (dT) (dT) -3'
siRNA control:	nothing	5'-UCUCUCACAACGGGCAU (dT) (dT) -3'
3'UTR from	sequence	
BMP2 (ED-miR-376a+b-3p binding site)	<p>CTCTCTCGAGGGAAAAAATAGCTAATTGTATTTATATGTAATCAAAAAGAGTATCGGGTTTGTACA TAATTTTCCAAAAATTGTAGTTGTTTTTCAGTTGTGTGTATTTAAGATGAAAAGTCTACATGGAAGGTTAC TCTGGCAAAGTGCTTAGCACGTTTGGCTTTTTTGCAGTGTACTGTTGAGTTCACAAGTTCAAGTCCAGAA AAAAAAGTGGATAATCCACTCTGCTGACTTTCAAGATTATATATTATTCAATTCTCAGGAATGTTGCA GAGTGATTGTCCAATCCATGAGAAATTTACATCCTTATTAGTTGGAATATTTGGATAAGAACCAGACATTG CTGATCTATTATAGAACTCTCCTCCTGCCCTTAATTTACAGAAAAGATAAAGCAGGATCCATAGAAAT AATTAGGAAAACGATGAACCTGCAGGAAAAGTGAATGATGGTTTGTGTTCTTCTTTCCATAATTAGTGAT CCCTTCAAAGGGCTGATCTGGCCAAAGTATTCATAAAAACGTAAGATTTCTTCATTATTGATATTGTGG TCATATATATTTGCGGCCCTTCC</p>	
BCL2 (ED-miR-376c-3p binding sites)	<p>CTCTCTCGAGTTTTTACATTATTAAGAAAAAAGATTTATTTATTTAAGACAGTCCCATCAAACTCCTG TCTTTGGAAATCCGACCCTAATTGCCAAGCACCGCTTCGTGTGGCTCCACCTGGATGTTCTGTGCCTGT AAACATAGATTTCGCTTTCCATGTTGTTGGCCGGATCACCATCTGAAGAGCAGACGGATGGAAAAAGGACC TGATCATTGGGGAAGCTGGCTTTCTGGCTGCTGGAGGCTGGGGAGAAGGTGTTCACTTCACTTGCATTTCT TTGCCCTGGGGATATTTAATGACAACCTTCTGGTTGGTAGGGACATCTGTTTCTAAATGTTTATTATGTA CAATACAGAAAAAATTTTATAAAAATTAAGCAATGTGAACTGAATTGGAGAGTGATAATACAAGTCCCT TAGTCTTACCAGTGAATCATTCTGTTCCATGTCTTTGGACAACCATGACCTTGGACAATCATGAAATAT GCATCTCACTGGATGCAAAGAAAATCAGATGGAGCATGAATGGTACTGTACCGGTTTCATCTGGACTGCC CAGAAAAATAACTTCAAGCAAACATCCTATGCGGCCGCGAG</p>	
BCL2 (ED-miR-381-3p binding sites)	<p>CTCTCTCGAGTATCATTATTTTTTACATTATTAAGAAAAAAGATTTATTTATTTAAGACAGTCCCA TCAAACTCCTGTCTTTGGAAATCCGACCCTAATTGCCAAGCACCGCTTCGTGTGGCTCCACCTGGATG TTCTGTGCCTGTAACATAGATTTCGCTTTCCATGTTGTTGGCCGGATCACCATCTGAAGAGCAGACGGAT GAAAGAGGACCTGATCATGGGGAAGCTGGCTTTCTGGCTGCTGGAGGCTGGGGAGAAGGTGTTCACTC ACTTGCATCTTTTGGCCCTGGGGGCTGTGATATTAACAGAGGGAGGGTTCTGTGGGGGAAGTCCATGC CTCCCTGGCCTGAAGAAGAGACTCTTTCGATATGACTCACATGATGCATACCTGGTGGGAGGAAAAGAGT TGGGAACCTCAGATGGACCTAGTACCCACTGAGATTTCCACGCCGAAGGACAGCGATGGGAAAAATGCC TTAAATCATAGGAAAGTATTTTTTTAAGCTACCAATTGTGCCGAGAAAAGCATTTTAGCAATTTATACAA TATCATCCAGTACCTTAAGCCCTGATTGCGGCCCTTCC</p>	
ANGPT2 (ED-miR-381-3p binding sites)	<p>CTCTCTCGAGACATCCCAGTCCACCTGAGGAACTGTCTCGAACTATTTTTCAAAGACTTAAGCCCAGTGCA CTGAAAGTCACGGCTGCGCACTGTGTCTCTTCCACCACAGAGGGCGTGTGCTCGGTGCTGACGGGACCC ACATGCTCCAGATTAGAGCCTGTAACTTTATCACTTAACTTGCATCACTTAACGGACCAAGCAAGAC CCTAAACATCCATAATTGTGATTAGACAGAACACCTATGCAAAGATGAACCCGAGGCTGAGAATCAGACT GACAGTTTACAGACGCTGCTGTACACAACCAAGAATGTTATGTGCAAGTTTATCAGTAAATAACTGGAAAA CAGAACACTTTATTATACATTTATTAGCCTTAGCAGGCAATAAACCAGAATCACTTTGAAGACACAGCA AAAAGTGATACACTCCGAGATCTGAAATAGATGTGTTCTCAGACAACAAAGTCCCTTCCAGAAATCTTCAT GTTCGATAAATGTTATGAATATTAACAAgAAGTTGATTGAGAAAGCGGCCGCGAG</p>	

Gray highlighted sequences are non-endogenous extensions containing restriction enzyme sites for cloning. Bold highlights indicate miRNA binding sites.

SUPPLEMENTAL REFERENCES

1. Pfaffl, MW (2001). A new mathematical model for relative quantification in real-time RT-PCR. *Nucleic Acids Res* **29**: e45.
2. Wu, D, Lim, E, Vaillant, F, Asselin-Labat, ML, Visvader, JE, and Smyth, GK (2010). ROAST: rotation gene set tests for complex microarray experiments. *Bioinformatics (Oxford, England)* **26**: 2176-2182.
3. Zheng, Y, Li, T, Ren, R, Shi, D, and Wang, S (2014). Revealing editing and SNPs of microRNAs in colon tissues by analyzing high-throughput sequencing profiles of small RNAs. *BMC Genomics* **15 Suppl 9**: S11.
4. Li, L, Song, Y, Shi, X, Liu, J, Xiong, S, Chen, W, Fu, Q, Huang, Z, Gu, N, and Zhang, R (2018). The landscape of miRNA editing in animals and its impact on miRNA biogenesis and targeting. *Genome Res* **28**: 132-143.
5. Pinto, Y, Buchumenski, I, Levanon, EY, and Eisenberg, E (2018). Human cancer tissues exhibit reduced A-to-I editing of miRNAs coupled with elevated editing of their targets. *Nucleic Acids Res* **46**: 71-82.
6. Su, Q, Li, L, Zhao, J, Sun, Y, and Yang, H (2017). MiRNA Expression Profile of the Myocardial Tissue of Pigs with Coronary Microembolization. *Cellular physiology and biochemistry : international journal of experimental cellular physiology, biochemistry, and pharmacology* **43**: 1012-1024.
7. Chiang, HR, Schoenfeld, LW, Ruby, JG, Auyeung, VC, Spies, N, Baek, D, Johnston, WK, Russ, C, Luo, S, Babiarz, JE, *et al.* (2010). Mammalian microRNAs: experimental evaluation of novel and previously annotated genes. *Genes & development* **24**: 992-1009.
8. Alon, S, Mor, E, Vigneault, F, Church, GM, Locatelli, F, Galeano, F, Gallo, A, Shomron, N, and Eisenberg, E (2012). Systematic identification of edited microRNAs in the human brain. *Genome Res* **22**: 1533-1540.
9. Ekdahl, Y, Farahani, HS, Behm, M, Lagergren, J, and Ohman, M (2012). A-to-I editing of microRNAs in the mammalian brain increases during development. *Genome Res* **22**: 1477-1487.
10. Korkmaz, G, le Sage, C, Tekirdag, KA, Agami, R, and Gozuacik, D (2012). miR-376b controls starvation and mTOR inhibition-related autophagy by targeting ATG4C and BECN1. *Autophagy* **8**: 165-176.
11. Gong, J, Wu, Y, Zhang, X, Liao, Y, Sibanda, VL, Liu, W, and Guo, AY (2014). Comprehensive analysis of human small RNA sequencing data provides insights into expression profiles and miRNA editing. *RNA Biol* **11**: 1375-1385.
12. Wang, Y, Xu, X, Yu, S, Jeong, KJ, Zhou, Z, Han, L, Tsang, YH, Li, J, Chen, H, Mangala, LS, *et al.* (2017). Systematic characterization of A-to-I RNA editing hotspots in microRNAs across human cancers. *Genome Res* **27**: 1112-1125.
13. Edelstein, LC, Simon, LM, Montoya, RT, Holinstat, M, Chen, ES, Bergeron, A, Kong, X, Nagalla, S, Mohandas, N, Cohen, DE, *et al.* (2013). Racial differences in human platelet PAR4 reactivity reflect expression of PCTP and miR-376c. *Nat Med* **19**: 1609-1616.
14. Liu, L, Yao, J, Li, Z, Zu, G, Feng, D, Li, Y, Qasim, W, Zhang, S, Li, T, Zeng, H, *et al.* (2018). miR-381-3p knockdown improves intestinal epithelial proliferation and barrier function after intestinal ischemia/reperfusion injury by targeting nurr1. *Cell death & disease* **9**: 411.
15. Stather, PW, Sylvius, N, Sidloff, DA, Dattani, N, Verissimo, A, Wild, JB, Butt, HZ, Choke, E, Sayers, RD, and Bown, MJ (2015). Identification of microRNAs associated with abdominal aortic aneurysms and peripheral arterial disease. *The British journal of surgery* **102**: 755-766.
16. Welten, SM, Goossens, EA, Quax, PH, and Nossent, AY (2016). The multifactorial nature of microRNAs in vascular remodelling. *Cardiovascular research* **110**: 6-22.

17. Xiang, Y, Guo, J, Peng, YF, Tan, T, Huang, HT, Luo, HC, and Wei, YS (2017). Association of miR-21, miR-126 and miR-605 gene polymorphisms with ischemic stroke risk. *Oncotarget* **8**: 95755-95763.
18. McManus, DD, and Freedman, JE (2015). MicroRNAs in platelet function and cardiovascular disease. *Nature reviews Cardiology* **12**: 711-717.
19. van der Kwast, RVCT, van Ingen, E, Parma, L, Peters, HAB, Quax, PHA, and Nossent, AY (2018). Adenosine-to-Inosine Editing of MicroRNA-487b Alters Target Gene Selection After Ischemia and Promotes Neovascularization. *Circ Res* **122**: 444-456.
20. Welten, SM, Bastiaansen, AJ, de, JR, de Vries, MR, Peters, EH, Boonstra, M, Sheikh, SP, La, MN, Kandimalla, ER, Quax, PH, *et al.* (2014). Inhibition of 14q32 MicroRNAs miR-329, miR-487b, miR-494 and miR-495 Increases Neovascularization and Blood Flow Recovery after Ischemia. *Circ Res*.
21. Romaine, SP, Tomaszewski, M, Condorelli, G, and Samani, NJ (2015). MicroRNAs in cardiovascular disease: an introduction for clinicians. *Heart (British Cardiac Society)* **101**: 921-928.
22. Lin, Z, Ge, J, Wang, Z, Ren, J, Wang, X, Xiong, H, Gao, J, Zhang, Y, and Zhang, Q (2017). Let-7e modulates the inflammatory response in vascular endothelial cells through ceRNA crosstalk. *Scientific reports* **7**: 42498.
23. Condorelli, G, Latronico, MV, and Cavarretta, E (2014). microRNAs in cardiovascular diseases: current knowledge and the road ahead. *J Am Coll Cardiol* **63**: 2177-2187.
24. Feinberg, MW, and Moore, KJ (2016). MicroRNA Regulation of Atherosclerosis. *Circ Res* **118**: 703-720.
25. Li, HW, Meng, Y, Xie, Q, Yi, WJ, Lai, XL, Bian, Q, Wang, J, Wang, JF, and Yu, G (2015). miR-98 protects endothelial cells against hypoxia/reoxygenation induced-apoptosis by targeting caspase-3. *Biochem Biophys Res Commun* **467**: 595-601.
26. Bao, MH, Li, JM, Luo, HQ, Tang, L, Lv, QL, Li, GY, and Zhou, HH (2016). NF-kappaB-Regulated miR-99a Modulates Endothelial Cell Inflammation. *Mediators of inflammation* **2016**: 5308170.
27. Olson, EN (2014). MicroRNAs as therapeutic targets and biomarkers of cardiovascular disease. *Science translational medicine* **6**: 239ps233.
28. Wang, X, Suofu, Y, Akpınar, B, Baranov, SV, Kim, J, Carlisle, DL, Zhang, Y, and Friedlander, RM (2017). Systemic antimir-337-3p delivery inhibits cerebral ischemia-mediated injury. *Neurobiology of disease* **105**: 156-163.
29. Marchand, A, Proust, C, Morange, PE, Lompre, AM, and Tregouet, DA (2012). miR-421 and miR-30c inhibit SERPINE 1 gene expression in human endothelial cells. *PLoS One* **7**: e44532.
30. Shoshan, E, Mobley, AK, Braeuer, RR, Kamiya, T, Huang, L, Vasquez, ME, Salameh, A, Lee, HJ, Kim, SJ, Ivan, C, *et al.* (2015). Reduced adenosine-to-inosine miR-455-5p editing promotes melanoma growth and metastasis. *Nat Cell Biol* **17**: 311-321.
31. Voellenkle, C, Rooij, J, Guffanti, A, Brini, E, Fasanaro, P, Isaia, E, Croft, L, David, M, Capogrossi, MC, Moles, A, *et al.* (2012). Deep-sequencing of endothelial cells exposed to hypoxia reveals the complexity of known and novel microRNAs. *Rna* **18**: 472-484.
32. Su, SH, Wu, CH, Chiu, YL, Chang, SJ, Lo, HH, Liao, KH, Tsai, CF, Tsai, TN, Lin, CH, Cheng, SM, *et al.* (2017). Dysregulation of Vascular Endothelial Growth Factor Receptor-2 by Multiple miRNAs in Endothelial Colony-Forming Cells of Coronary Artery Disease. *Journal of vascular research* **54**: 22-32.
33. Hui, J, Huishan, W, Tao, L, Zhonglu, Y, Renteng, Z, and Hongguang, H (2017). miR-539 as a key negative regulator of the MEK pathway in myocardial infarction. *Herz* **42**: 781-789.
34. Qiang, L, Hong, L, Ningfu, W, Huaihong, C, and Jing, W (2013). Expression of miR-126 and miR-508-5p in endothelial progenitor cells is associated with the prognosis of chronic heart failure patients. *International journal of cardiology* **168**: 2082-2088.

35. Cheuk, BL, and Cheng, SW (2014). Identification and characterization of microRNAs in vascular smooth muscle cells from patients with abdominal aortic aneurysms. *Journal of vascular surgery* **59**: 202-209.
36. Agarwal, V, Bell, GW, Nam, JW, and Bartel, DP (2015). Predicting effective microRNA target sites in mammalian mRNAs. *eLife* **4**.
37. Mi, H, Huang, X, Muruganujan, A, Tang, H, Mills, C, Kang, D, and Thomas, PD (2017). PANTHER version II: expanded annotation data from Gene Ontology and Reactome pathways, and data analysis tool enhancements. *Nucleic Acids Res* **45**: D183-D189.
38. Ritchie, ME, Phipson, B, Wu, D, Hu, Y, Law, CW, Shi, W, and Smyth, GK (2015). limma powers differential expression analyses for RNA-sequencing and microarray studies. *Nucleic Acids Res* **43**: e47.